Redox Biology 37 (2020) 101754

Contents lists available at ScienceDirect

Redox Biology

journal homepage: www.elsevier.com/locate/redox

Research Paper

Methylation-dependent antioxidant-redox imbalance regulates hypertensive kidney injury in aging

Sathnur Pushpakumar [a,1], Lu Ren [b,1], Subir Kumar Juin [a], Suravi Majumder [a], Rohan Kulkarni [a], Utpal Sen [a,*]

[a] Department of Physiology, University of Louisville School of Medicine, Louisville, KY, USA
[b] Department of Cancer Biology, University of Cincinnati College of Medicine, Cincinnati, OH, USA

ARTICLE INFO

Keywords:
Hypertension
Aging
Kidney
Epigenetics
Oxidase
Catalase
Nox4
Sirt
DNMT

ABSTRACT

The prevalence of hypertension increases with age, and oxidative stress is a major contributing factor to the pathogenesis of hypertension-induced kidney damage in aging. The nicotinamide adenine dinucleotide phosphate (NADPH) family is one of the major sources of reactive oxygen species (ROS) generation, and several NADPH oxidase isoforms are highly expressed in the kidney. Although epigenetic protein modification plays a role in organ injury, the methylation of the oxidant-antioxidant defense system and their role in hypertension-induced kidney damage in aging remains underexplored. The present study investigated the role of NADPH oxidase 4, superoxide dismutases (SODs), catalase, and NOS in Ang-II induced kidney damage in aging. Wild type (WT, C57BL/6J) mice aged 12–14 and 75–78 weeks were used and treated with or without Ang-II (1000 ng/kg/min) for 4 weeks with control mice receiving saline. Aged mice with or without Ang-II exhibited higher mean BP, lower renal blood flow, and decreased renal vascular density compared to young mice. While superoxide, 4-HNE, $p22^{phox}$, Nox4, iNOS were increased in the aged kidney, the expression of eNOS, MnSOD, CuSOD, catalase, Sirt1, and -3 as well as the ratio of GSH/GSSG, and activities of SODs and catalase were decreased compared to young control mice. The changes further deteriorated with Ang-II treatment. In Ang-II treated aged mice, the expressions of DNMTs were increased and associated with increased methylation of SODs, Sirt1, and Nox4. We conclude that hypermethylation of antioxidant enzymes in the aged kidney during hypertension worsens redox imbalance leading to kidney damage.

1. Introduction

Hypertension is the second leading cause of kidney failure in the US, as well as chronic kidney disease (CKD) in the world [1]. It is also a significant risk factor for cardiovascular events, including stroke and heart attack resulting in increased morbidity and mortality globally [2]. Earlier evidence indicated a correlation between aging and the development of hypertension involving several key pathophysiological mechanisms, including inflammation, oxidative stress, and endothelial dysfunction [3]. While the pathophysiological processes and the cause of hypertension in aging are multifactorial and complex, the organ injury remains a universal occurrence. Despite substantial efforts to identify a specific and manageable target(s), the vast majority of treatments failed to bring a major breakthrough. Thus, hypertensive organ injury remains a persistent challenge to achieve desired health benefits in the elderly population.

The dynamics of aging is a multifaceted process that occurs by irreversible changes of biological and physiological processes by various factors including environmental effects and epigenetics [4]. Besides, gradual loss of hemodynamic mechanisms in aging also attributes to molecular disorders, for example, oxidative damage from increased reactive oxygen species (ROS) [5]. The level of ROS increases when the endogenous antioxidant mechanisms are deficient, and thus changes the cellular environment from normal redox state to heightened oxidative stress [6]. The elevated oxidative stress increases exponentially with age, which is paralleled by a dramatic decrease in the cell repair machinery [7]. Clinical studies demonstrate that age is a main non-modifiable risk factor in hypertension development due to the

* Corresponding author. Department of Physiology, 500 South Preston Street. HSC-A, Room 1115, University of Louisville School of Medicine, Louisville, KY, 40202, USA.
E-mail address: u0sen001@louisville.edu (U. Sen).
[1] These authors contributed equally.

https://doi.org/10.1016/j.redox.2020.101754
Received 19 March 2020; Received in revised form 20 August 2020; Accepted 8 October 2020
Available online 10 October 2020

Table 1
Primer sequence for PCR.

Type	Forward sequence (5′-3′)	Reverse sequence (5′-3′)
MnSOD *(unmethylated)*	TTAATGTTATTGAGGAGAAGTATTATGA	AAAAACATTTATACAAACCAACAAA
MnSOD *(methylated)*	ACGTTATCGAGGAGAAGTATTACGA	AAAAAAACGTTTATACGAACCAACG
CuSOD *(unmethylated)*	TTTTAATTTTTATATTGTAATTGAGGTGTG	AAAAAACCTAAACAAAAAAAATCACT
CuSOD *(methylated)*	AATTTTTATATTGTAATCGAGGCGC	GAAAAACCTAAACGAAAAAAATCG
Nox4 *(unmethylated)*	ATGTGTTTTGGGATGTAAAGAATGT	TATCTCACACAAACCTATTATTATAACAAC
Nox4 *(methylated)*	GCGTTTCGGGATGTAAAGAAC	GCGCGAACCTATTATTATAACGAC
Sirt1 *(unmethylated)*	TTTGTTTTTGTTTTTTTTGTTTTGT	CATAACCCAACATATTATAATCCAAC
Sirt1 *(methylated)*	TTCGTTTTCGTTTTTTTTGTTTC	GTAACCCGACGTATTATAATCCG
GAPDH	GTCGTGGAGTCTACTGGTGT	TGCTGACAATCTTGAGTGAG

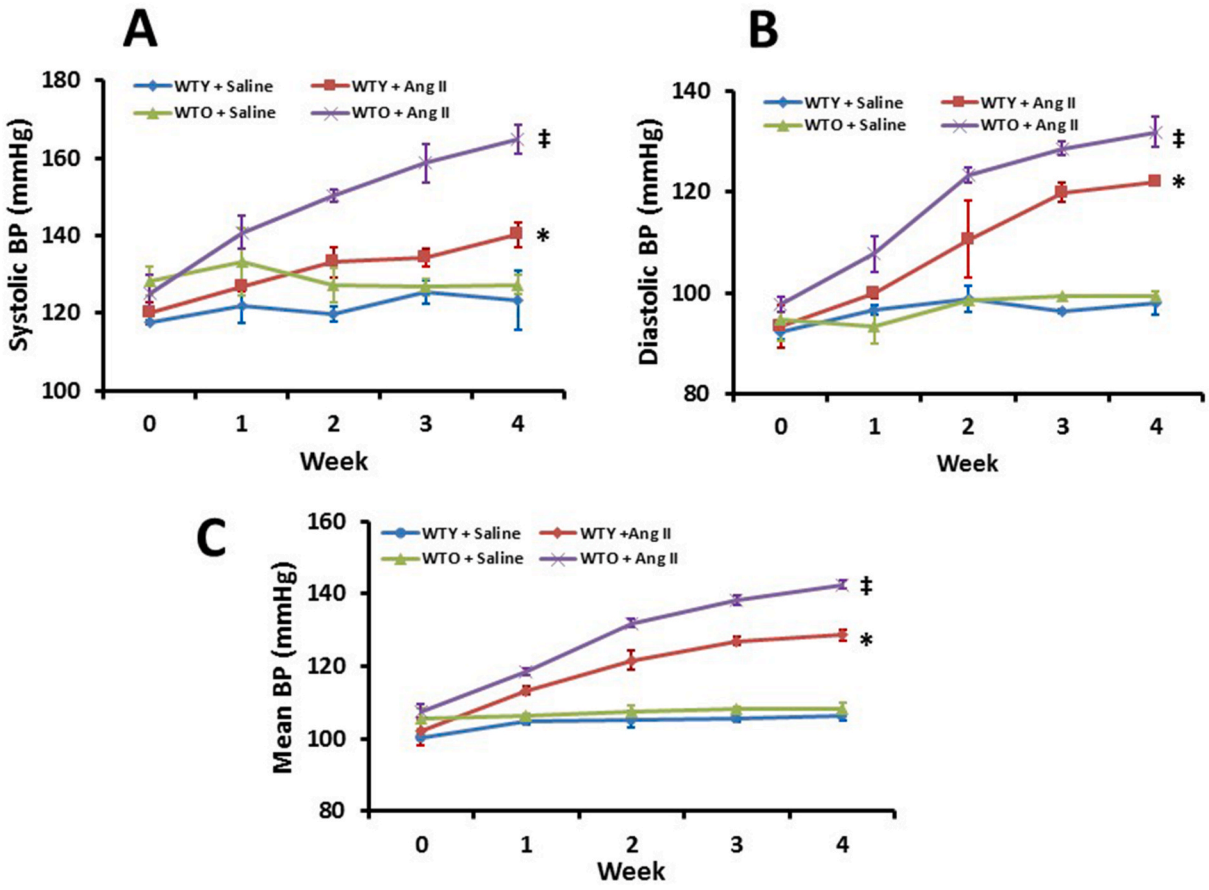

Fig. 1. Aged mice showed a higher susceptibility to develop hypertension than young mice in response to Ang-II. Systolic (A), diastolic (B), and mean (C) arterial blood pressure was measured by DSI radiotelemetry method. Values are presented as mean ± SD (n = 5). *p < 0.05 vs. WTY + Saline; ‡p < 0.05 vs. other groups.

alterations occurring in the vasculature, such as endothelial dysfunction, vascular remodeling, increased vascular stiffness, and inflammation [8]. Thus, the prevalence of hypertension rises with age.

Although oxidative stress plays a crucial role in the development of hypertension-induced vascular damage and dysfunction [9], the underlying mechanisms are still ill-defined. In kidney vasculature, glomerular and tubular epithelial cells are susceptible to oxidative stress-induced damage [10]. Further, stress-induced mesangial and endothelial cell damage leads to morphological changes in the glomeruli and functional impairment [11]. The main components of ROS are superoxide ($O_2^{\bullet -}$), hydrogen peroxide (H_2O_2), and peroxynitrite ($ONOO^{\bullet -}$). In the body, several enzymes, including nicotinamide adenine dinucleotide (NADH), nicotinamide adenine dinucleotide phosphate (NADPH) oxidase, and nitric oxide synthase (NOS) produce ROS either directly or through a secondary oxidative pathway. For example, though the main function of NOS enzymes is to catalyze the production of NO from L-arginine, overproduction of NO in an oxidative environment can have serious consequences as NO reacts with oxidative radicals to produce powerful oxidant, peroxynitrite ($ONOO^-$).

NADPH oxidase is a family of enzymes that are the main source of

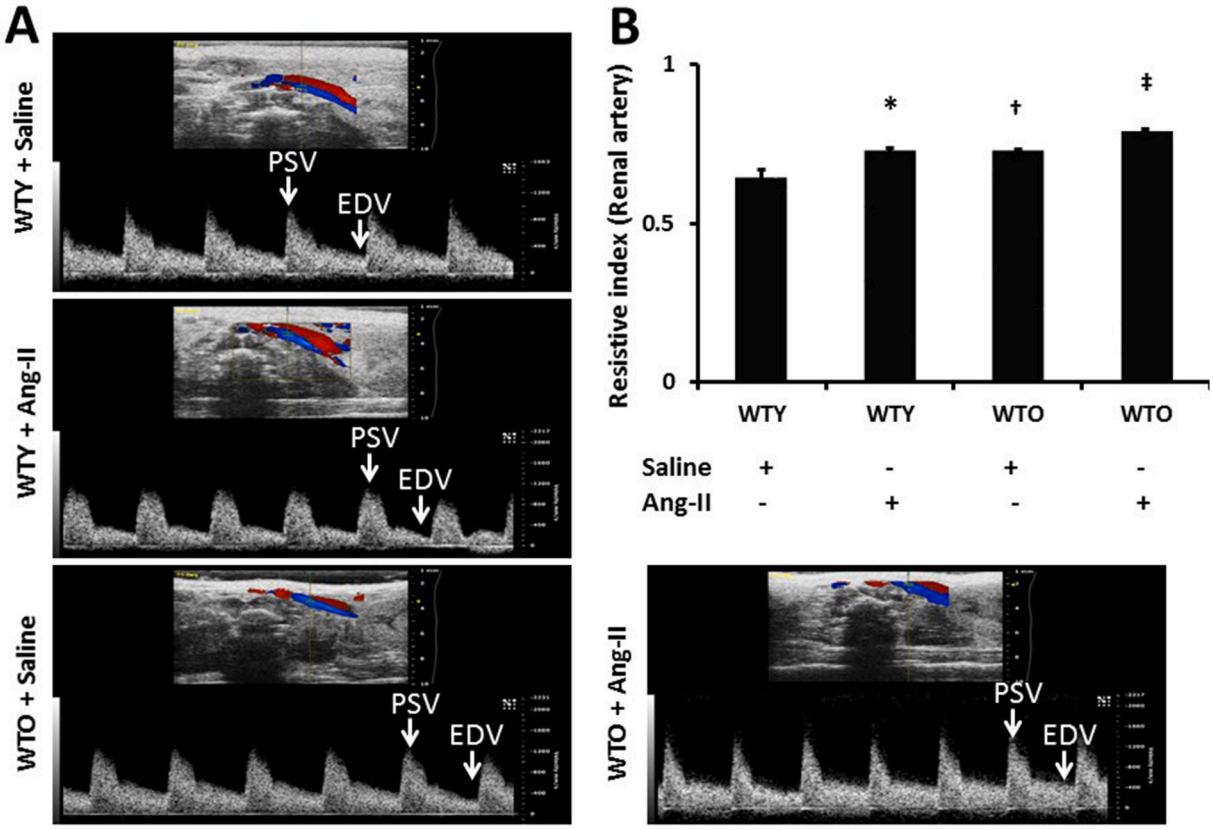

Fig. 2. Echographic determination of mean renal arterial blood velocity in WTY and WTO mice treated with or without Ang-II and saline. (A) Representative waveforms of young and old mice treated without or with Ang-II and saline. Velocity was detected from pulsed Doppler waveforms acquired from renal artery in isoflurane-anesthetized mice. (B) Resistive index (RI) was calculated as (PSV - EDV)/PSV, using Vevo 2100 Workstation Software. Bars are mean ± SD (n = 5). *, †$p < 0.05$ vs. WTY + Saline; ‡$p < 0.05$ vs. other groups.

ROS in the renal vasculature [12]. The members of NADPH family include Nox1, Nox2, Nox3, Nox4, and Nox5 based on their homologies [13]. Nox4 is unique among the other isoforms and is found in the plasma membrane, focal adhesions, nucleus, mitochondria, and endoplasmic reticulum along with other cellular components [14]. Although increased renal Nox4 was shown to be associated with increased ROS production in renal proximal tubular cells [15], the role of Nox4 in renal injury during hypertension in aging is not clear.

While ROS causes cellular damage, superoxide dismutases (SODs), such as MnSOD and CuSOD, and catalase suppress or prevent the formation of free radicals, and are considered as the first-line antioxidant defense system [16]. The enzymes are responsible for dismuting superoxide and breakdown of H_2O_2 to harmless molecules, H_2O and O_2. On the other hand, Sirtuins are NAD^+-dependent histone deacetylases, and recent studies suggest that Sirt1 and Sirt3 play a key role in protecting cells from oxidative stress by decreasing ROS production [17,18]. Therefore, the disruption of the delicate balance between catalase, SODs, Sirt1, -3, and oxygen radical producing enzymes alters the normal redox state to modify proteins leading to organ damage in age-associated hypertension.

In addition to redox imbalance, epigenetic alterations that include DNA methylation can mediate redox signaling and contribute to vascular disease progression such as, salt-sensitive hypertension [19]. Studies have indicated an association between hypertension with a loss of global genomic DNA methylation [20], in which modification of histones play a variety of role in hypertensive disorders. However, whether epigenetic changes leads to redox imbalance through DNA methylation and contributes to hypertensive kidney injury in aging has not been fully explored. In this study, we investigated whether epigenetic modulation of the oxidant-antioxidant system contributes to aging kidney injury and dysfunction in Ang-II-hypertension.

2. Materials and methods

2.1. Antibodies and reagents

Sirt3, 4-HNE, Alexa Fluor 488 Goat Anti-Rabbit, Alexa Fluor 594 Anti-Rabbit, Alexa Fluor 488 Anti-Mouse, Alexa Fluor 594 Anti-Mouse antibodies (Cat. Nos.: PA586035, MA527570, A-11008, A-11012, A-11001, A-11005, respectively), and Dihydroethidium (Cat. No.: D11347) were from Thermo Fisher Scientific (Carlsbad, CA). Nox4, $p22^{phox}$, Catalase, β-Actin antibodies (Cat. Nos.: sc-55142, sc-20781, sc-50508, sc-47778 HRP, respectively) were from Santa Cruz Biotechnology (Dallas, TX). MnSOD antibody (Cat. No.: 06–984) was from MilliporeSigma (Burlington, MA). Antibodies against iNOS and eNOS (Cat. Nos.: 610329 and 610297, respectively) were from BD Biosciences (San Jose, CA). DNA methyltransferase (DNMT) 1, 3a, 3b antibodies (Cat. Nos.: ab13537, ab13888, and ab13604, respectively) and GSH/GSSG Ratio detection kit (Cat. No.: ab138881) were from Abcam (Cambridge, UK). Anti-Sirt1 antibody (Cat. No.: 8469) was from Cell Signaling Technology (Danvers, MA), and Superoxide dismutase and Catalase assay kits (Cat. Nos.: 706002 and 707002, respectively) were from Cayman Chemicals (Ann Arbor, MI).

2.2. Animals and groups

All animal procedures were performed according to institutional animal care and use committee approved protocols of the University Of Louisville School Of Medicine and conformed to the *Guide for the Care and Use of Laboratory Animals* published by the U.S. National Institutes of

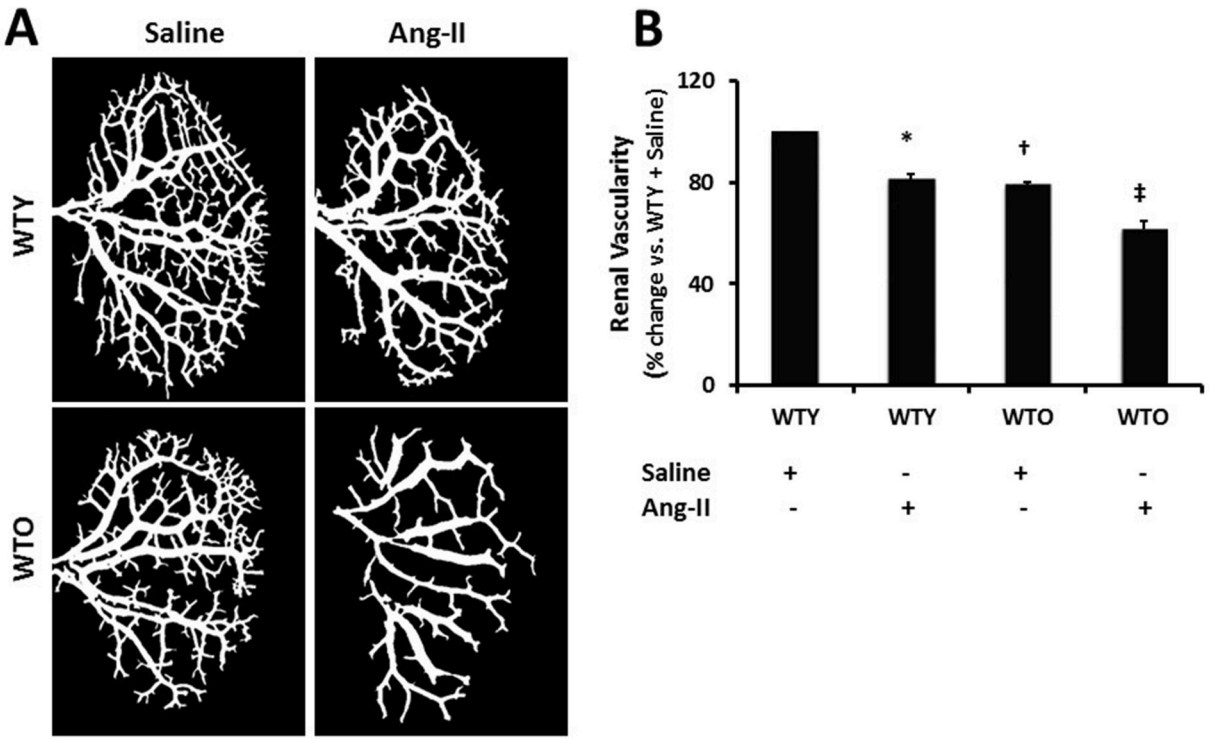

Fig. 3. Ang-II treatment attenuated vascular density. Renal vascular architecture was captured by Carestream Molecular Imaging In-vivo Multispectral system after infusion of 0.6 ml of barium sulfate (0.1 mg/ml) in the infrarenal aorta through a PE10 tube. (A) Vascular density was quantified utilizing Vessel Segmentation software. (B) Bar diagram represents the mean percentage change ± SD (n = 5). Values were obtained after background subtraction and plotted as percent change from WTY + saline group (100%). *, †$p < 0.05$ vs. WTY + Saline; ‡$p < 0.05$ vs. other groups.

Health (NIH Publication, 2011).

C57BL/6J (wild-type, WT) mice were purchased from Jackson Laboratory (Bar Harbor, ME). Mice aged 12–14 weeks were used as young and 75–78 weeks as old in this study. The animals were fed standard chow and water ad libitum. The animals were treated with Angiotensin-II (1000 ng/kg/min) or saline for 4-week period. Blood pressure was determined by DSI radiotelemetry method at 0, 1, 2, 3 and 4 weeks using a pressure transducer (PA-C10) (Data Sciences International; St. Paul, MN) as described before [21].

2.3. Renal ultrasound

Ultrasonography was carried out to measure the blood flow in the renal cortex, as described before [22]. Briefly, the animals were anesthetized by isoflurane inhalation and placed supine on a heated platform at 37.5 °C. After depilation, imaging was obtained using Vevo 2100 system (VisualSonics, Toronto, ON, Canada). The transducer, MS550D (22–55 MHz), was focused on vessels of the left kidney and scanned in the short axis. Peak systolic velocity (PSV) and end-diastolic velocity (EDV) (mm/sec) of blood flow in the Pulsed-Wave Doppler mode were recorded. Cine loops were exported and analyzed to calculate the renal cortical artery resistive index (RI).

2.4. Cortical blood flow measurement

Renal arterial and cortical blood flow were detected by using Speckle Contrast Imager (Moor FLPI, Wilmington, DE), as described before [23]. A dorsal incision was used to expose and focus the camera on the aorta, renal artery, vein, and the kidney to obtain cortical flux units (No. of RBCs x velocity).

2.5. Barium angiography

Renal vascular density was assessed by barium angiography, as described previously [23]. The left kidney was infused with barium sulfate solution (0.1 g/mL) via PE10 catheter (ID - 0.28 mm; Franklin Lake, NJ) inserted into the infrarenal aorta. The images were captured by Carestream Molecular Imaging In vivo Multispectral System (Rochester, NY). Vessel density was quantified using Vessel Segmentation and Analysis software (https://www.isip.uni-luebeck.de/downloads/vessel-segmentation-and-analysis.html).

2.6. Superoxide ($O_2^{\bullet-}$) detection

Frozen sections (5 μm thickness) were washed with PBS and stained with 5 μM/L dihydroethidium (DHE; Invitrogen, Carlsbad, Calif, USA) for 10 min in the dark humidified chamber. The fluorescence images were captured by Olympus FluoView1000 laser scanning confocal microscope (B&B Microscope, Pittsburg, PA).

2.7. Western blotting

Kidney tissue homogenates were partitioned on SDS-PAGE, electrophoretically separated, and transferred overnight to Polyvinylidine difluoride (PVDF) membrane. The membranes were blocked with 5% non-fat dry milk in PBS-T for 1 h, washed, and incubated with appropriate primary antibodies overnight at 4 °C. The membrane was washed to remove primary antibody and incubated with corresponding HRP-conjugated secondary antibody for 2 h at room temperature. Immunoreactive bands were developed using chemiluminescence and visualized under ChemiDoc MP System (BioRad). Band intensities were quantified using ImageJ software, as described earlier [24].

2.8. Detection of GSH: GSSG ratio

GSH/GSSG was quantified using GSH/GSSG ratio detection assay kit (refer antibodies and reagents section). Briefly, samples were homogenized in PBS/0.5% NP-40 buffer (pH 6). After deproteinization with

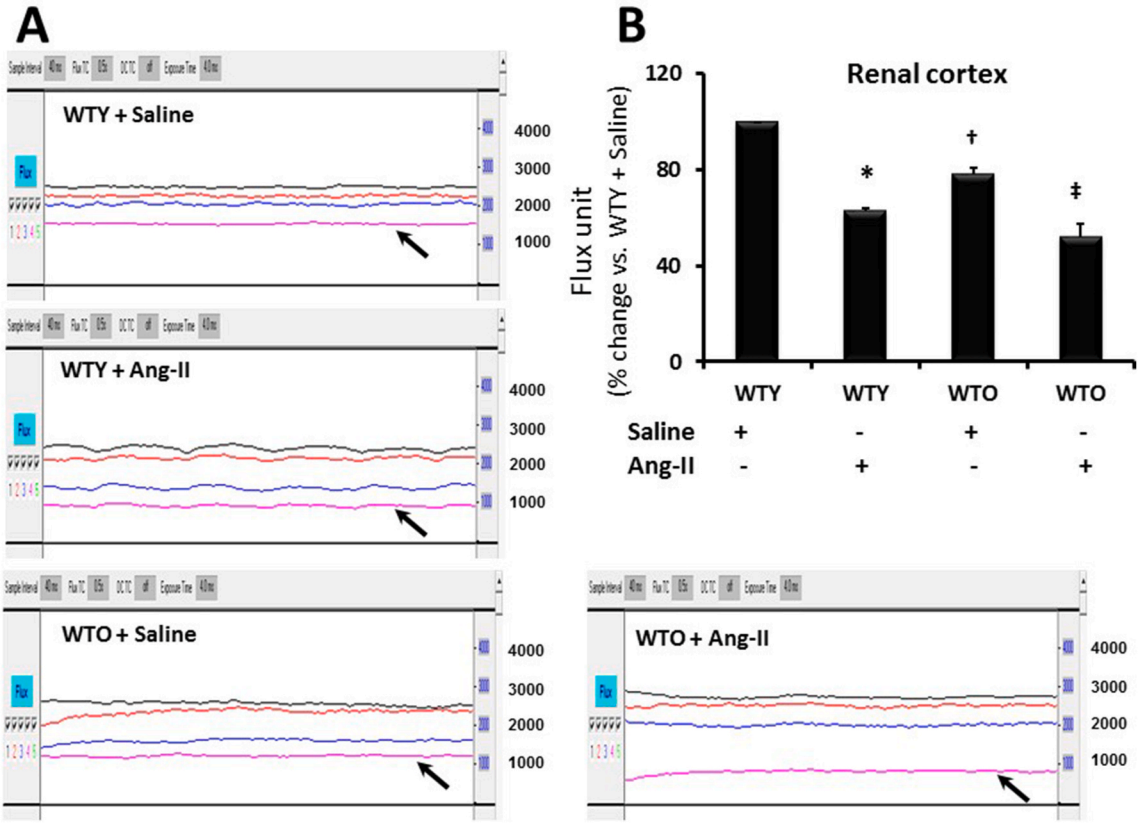

Fig. 4. Ang-II-hypertension reduced renal cortical blood flow in young and old mice. (A) Line figure showing laser Doppler flowmetry data (flux units: no. of RBCs × velocity) in the aorta (black trace), renal artery (red trace), renal vein (blue trace), and renal cortex (pink trace, black arrow). (B) The bar graph represents the mean flux units as the percent change in the renal cortex ± SD (n = 5). Values among the groups were calculated and plotted using WTY + saline flux units as 100%. *, †$p < 0.05$ vs. WTY + Saline; ‡$p < 0.05$ vs. other groups. (For interpretation of the references to color in this figure legend, the reader is referred to the Web version of this article.)

Trichloroacetic acid, samples were neutralized with $NaHCO_3$ to pH 4–6. The assay and data analysis was done following the manufacturer's instructions. The fluorescence was measured at EX/EM = 490/520 using SpectraMax M2e (Molecular Devices, Sunnyvale, CA).

2.9. Immunostaining

The frozen kidney was sectioned at a thickness of 5 μm and fixed with a fresh 4% paraformaldehyde for 20 min. After blocking for 45 min at room temperature, sections were incubated with appropriate primary antibodies overnight at 4 °C. Immune labeling was continued by incubating appropriate Alexa Fluor 488 and/or 594 conjugated secondary antibodies (Invitrogen, Carlsbad, CA) for 90 min at room temperature. Images were taken using Olympus FluoView1000 laser scanning confocal microscope (B&B Microscope, Pittsburg, PA). Fluorescent intensity was quantified using ImageJ software, as described earlier.

2.10. Catalase assay

Catalase activity was measured by using a Catalase Assay kit (refer antibodies and reagents section) following the manufacturer's instructions. Briefly, the samples were homogenized with phosphate buffer. In the presence of optimal H_2O_2, catalase oxidizes methanol to generate formaldehyde. The concentration of the color product, 4-amino-3-hydrazino-5-mercapto-1,2,4-triazole, was measured at 540 nm by SpectraMax M2e (Molecular Devices, Sunnyvale, CA). The catalase activity was calculated using the formula: Formaldehyde (μM) = [Sample absorbance- (y-intercept)/Slope] x 0.17/0.02 mL. Catalase activity = (μM of sample/20 min) x sample dilution = nmol/min/ml.

2.11. SOD activity

The cytosolic and mitochondrial superoxide dismutase activity was measured using an assay kit (refer antibodies and reagents section) following the manufacturer's instructions. Briefly, kidneys were homogenized in ice-cold HEPES buffer containing EGTA (1 mM), mannitol (210 mM), and sucrose (70 mM). The assay measures the reduction of Tetrazolium salt to Formazan in the presence of superoxide radicals generated by Xanthine oxidase and hypoxanthine. The absorbance was measured at 450 nm using SpectraMax M2e (Molecular Devices, Sunnyvale, CA). The total and MnSOD activity was calculated using the formula: SOD (U/ml) = [(Sample linearized absorbance – y-intercept)/(Slope) x (0.23/0.01) ml.

2.12. DNMT activity assay

DNMT (DNA methyltransferase) activity was measured as described before [25]. Briefly, nuclear proteins were extracted from the kidney using EpiQuick kit (Epigentek, Farmingdale, NY). The enzyme activity was measured using EpiQuik DNMT Activity/Inhibition Assay Ultra kit (Epigentek). All samples (20 μg nuclear extracts) were incubated in a plate coated with DNMT substrate followed by the addition of S-adenosylmethionine (SAM) in assay buffer at 37 °C for 90 min. Blank wells had SAM and substrate, and positive controls had substrate/SAM/purified DNMT enzyme. The capture antibody and detection solution were added in sequence followed by incubation for 60 and 50 min respectively. After washes, the developer solution was added, and the reaction was terminated by stop solution after color development. Absorbance was read at 450 and 655 nm on a microplate reader

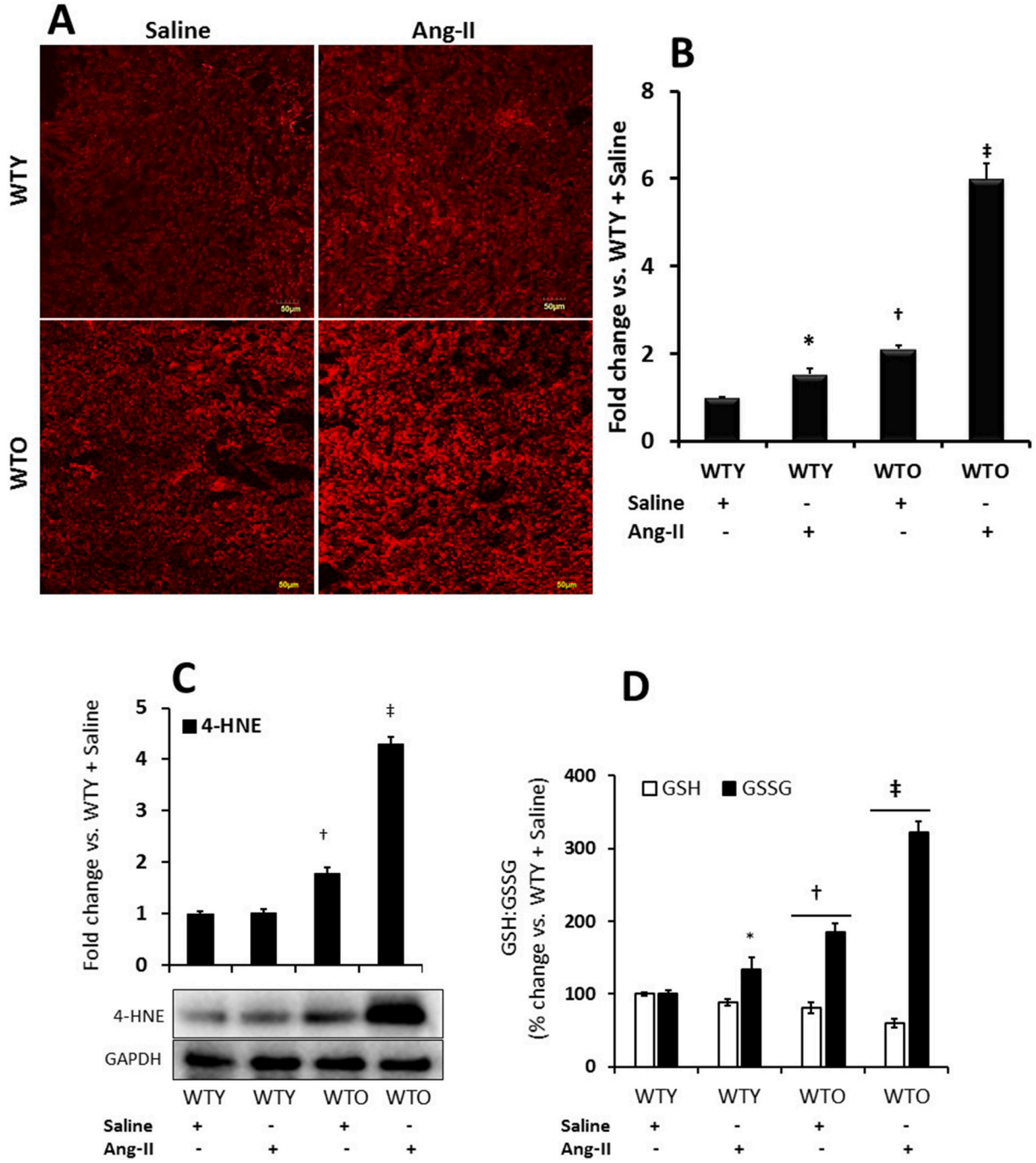

Fig. 5. Ang-II treatment increased oxidative stress in aged mice. (A) Superoxide radical anion ($O_2^{\bullet-}$) was measured in the kidney sections by applying the oxidative fluorescent dye, dihydroethidium (DHE). Images were acquired with a laser scanning confocal microscope using an appropriate filter (FluoView 1000; Olympus, Tokyo, Japan). (B) The bar graph represents the mean fold change of WTY ± SD (n = 5). *, †$p < 0.05$ vs. WTY + Saline; ‡$p < 0.05$ vs. other groups. Magnification, × 20. (C) 4-Hydroxynonenal (4-HNE), an α, β-unsaturated hydroxyalkenal product produced by lipid peroxidation was measured by Western blotting, and (D) reduced vs. oxidized glutathione (GSH: GSSG) was measured by an assay kit as described in the materials and methods. (C) and (D) The bar graphs represent the mean fold change of WTY ± SD (n = 5). *, †$p < 0.05$ vs. WTY + Saline; ‡$p < 0.05$ vs. other groups.

(SpectraMax M2; Molecular Devices, Sunnyvale, CA). The DNMT activity [optical density (OD)/h·mg] was calculated using DNMT activity = (sample OD − blank OD)/[protein amount (μg) × h] × 1000.

2.13. DNA methylation

Genomic DNA was extracted using Quick-gDNA MicroPrep (Zymo Research, Irvine, CA). Bisulfite conversion of gDNA was done using EZ DNA Methylation-Lightning Kit (Zymo Research) by following the manufacturer's protocol. Methylation-specific PCR was done to detect changes in Nox4, Sirt1, MnSOD, and CuSOD genes by specifically targeting converted (unmethylated) or unconverted (methylated) CpG sites. The primer sequences used are presented in Table 1. Products were run on 1.5% agarose gel and bands visualized using ChemiDoc XRS system (Bo-Rad, Hercules, CA).

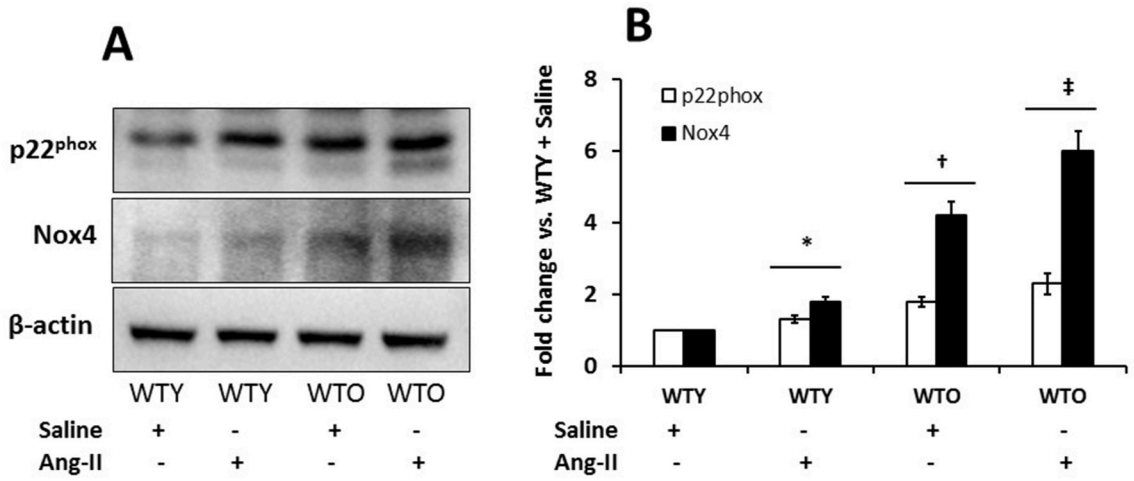

Fig. 6. Nox4 and p22^{phox} were highly upregulated in the aged hypertensive kidney. (A) Protein was isolated from the kidney tissue and was analyzed by Western blot. An equal amount of protein was loaded in each well, and the expression of each of the proteins was normalized with β-actin. The bands were quantified by densitometry analysis. (B) The bar graph represents the mean fold change ± SD (n = 5). Significant difference *, $^{\dagger}p < 0.05$ vs. WTY + Saline; $^{\ddagger}p < 0.05$ vs. other groups.

2.14. Statistical analysis

All data are expressed as mean ± SD. One-way analysis of variance (ANOVA) was used to analyze treatment effects, and differences between groups were determined by applying Tukey's post-hoc test. Significance was considered for a p-value of less than 0.05.

3. Results

3.1. Ang-II induced acute hypertension in aged mice

At the beginning of the experiments and until two weeks of treatment, the old mice receiving saline showed higher systolic blood pressure (SBP) compared to young littermate control (Fig. 1A). After two weeks, the SBP of young and old mice treated with saline showed non-significant changes but remained comparable thereafter until the end of 4-week experiment (Fig. 1A). The young mice treated with Ang-II showed higher SBP compared to the young saline control throughout the experimental period. In the old mice treated with Ang-II, the SBP increased steadily and significantly until the end-point of experiments compared to old mice treated with saline and young mice treated with Ang-II (Fig. 1A).

The diastolic blood pressure (DBP) of young and old mice with saline treatment was comparable and remained similar from baseline until the end of 4-week period (Fig. 1B). The DBP in both young and old mice increased with Ang-II until the end of experiments compared to their respective controls (Fig. 1B). The increase in DBP in old mice treated with Ang-II was significantly higher than DBP in young mice treated with Ang-II (Fig. 1B). The mean blood pressure (MBP) in all the four groups were similar to DBP changes. (Fig. 1C). Overall, the BP increment in aged mice was significantly higher than in young mice in response to Ang-II, suggesting increased susceptibility to Ang-II induced hypertension.

3.2. Hypertension aggravated renal artery resistive index (RI) in aged mice

Renal ultrasound was done to measure the blood flow velocities and determine the renal artery RI. The RI is used to assess the stiffness of vessels to blood flow and calculated as (PSV - EDV)/PSV. Fig. 2A are representative ultrasound Doppler images showing velocities in the renal artery of all four groups. Data indicated that WTY control mice had basal RI about 0.54 (Fig. 2A-B). After 4 weeks of Ang-II treatment, the RI increased to 0.62 in WTY compared to saline treated WTY mice. The RI of WTO control mice was higher than WTY control mice (0.61 vs. 0.54) and increased further with Ang-II treatment (0.69) (Fig. 2A-B). These results suggest that WTO mice exhibit excess renovascular resistance during Ang-II-induced hypertension than in young control littermates with Ang-II regimen.

3.3. Hypertensive aged mice showed reduced vascular density in the kidney

Barium sulfate angiography was done to determine changes in the renal vasculature. The renal vascular density in the young animals receiving saline treatment was considered normal (Fig. 3A). Upon Ang-II treatment, the renal vascular density was significantly decreased compared to saline treated young mice (Fig. 3A-B). Old saline-treated mice showed reduced vascular density, which was comparable to young Ang-II treated mice. Ang-II treatment further decreased the renal blood vessels in old mice compared to age-matched saline-treated mice and young mice groups (Fig. 3A-B).

3.4. Renal cortical blood flow declined in Ang-II-induced hypertension

The blood flow was evaluated by focusing the laser beam midway between the hilum and the outer edge of the kidney, and the data was recorded for 2 min. The renal cortical flux [number of red blood cells (RBCs) × velocity], as shown in Fig. 4, demonstrated the change of flow pattern between the animal groups. The young mice which received saline treatment had the basal level of renal blood flow (Fig. 4A-B). Ang-II treatment significantly reduced the cortical blood flow in young mice compared to age-matched control. In the saline treated old mice, blood flow was significantly decreased compared to young mice treated with saline (Fig. 4A-B). The blood flow was further decreased in the old animals treated with Ang-II compared to old mice treated with saline and young mice groups with or without Ang-II (Fig. 4A-B).

3.5. Ang-II hypertension aggravated renal oxidative stress in aged mice

Superoxide ($O_2^{\bullet-}$) radicals in the kidney sections were measured by DHE fluorescence assay, as described previously [24]. The fluorescence intensity in young control mice was considered as the baseline (Fig. 5A-B). The fluorescence intensity increased significantly in young mice receiving Ang-II compared to young control. In old mice receiving saline, the fluorescence level was significantly higher than in young

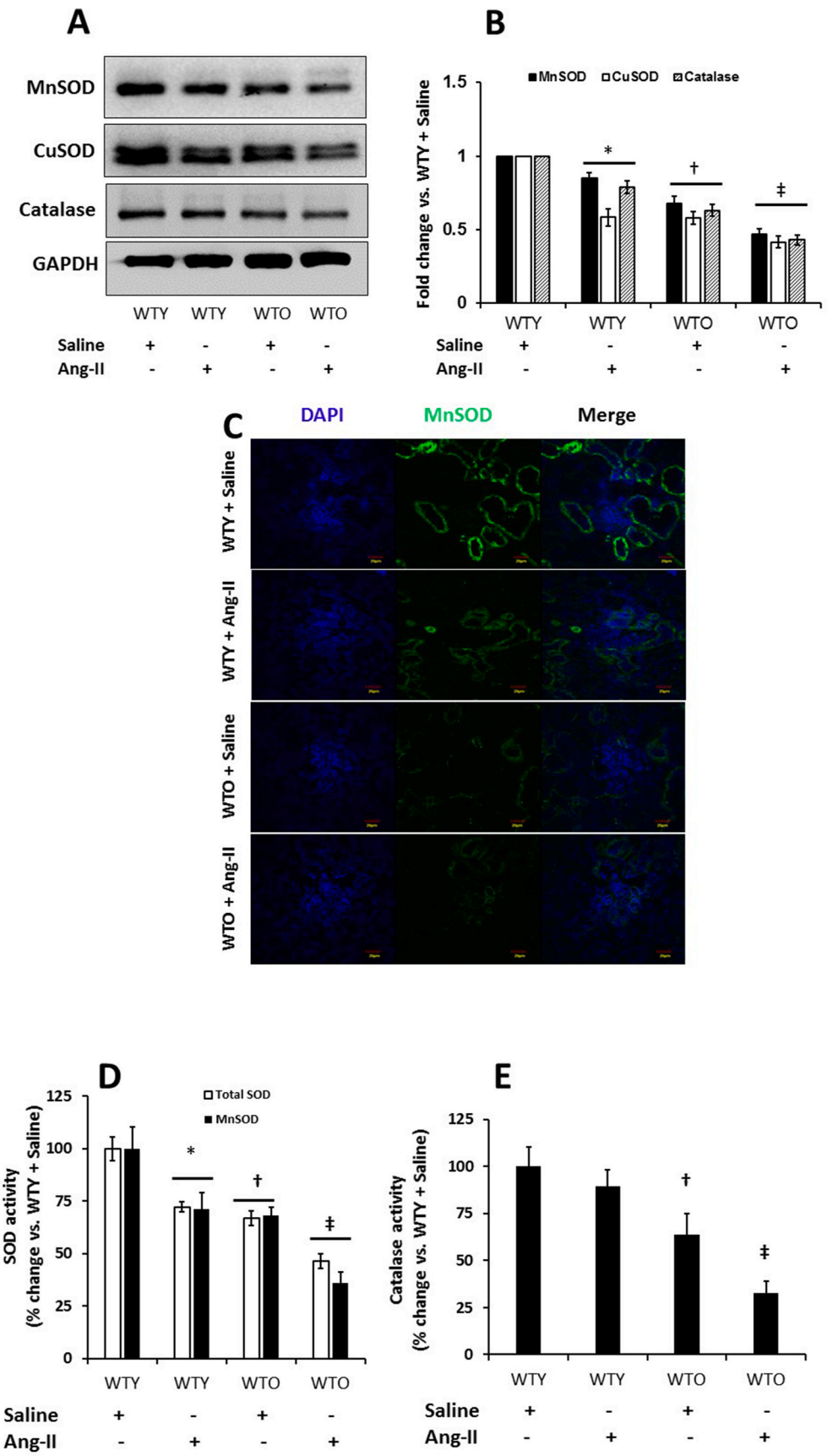

Fig. 7. Hypertension severely reduced expression of MnSOD, CuSOD, and Catalase in old mice. Western blot analysis of kidney tissue obtained from mice treated without or with Ang-II. (A) Bands are showing expression of MnSOD, CuSOD, and catalase in an equal amount of loaded proteins. Loading was normalized with GAPDH. (B) The bar diagrams indicate densitometric analysis of protein bands. Data represent mean fold change ± SD (n = 5). Significant difference *, †$p < 0.05$ vs. WTY + Saline; ‡$p < 0.05$ vs. other groups. (C) Immunostaining indicated MnSOD expression was lowest in the aged hypertensive kidney. Representative images of MnSOD fluorescence staining in the kidney section. (D) MnSOD, total SOD, and (E) Catalase activities were measured as described in the materials and methods. Data represent mean percent change ± SD (n = 5). Significant difference *, †$p < 0.05$ vs. WTY + Saline; ‡$p < 0.05$ vs. other groups.

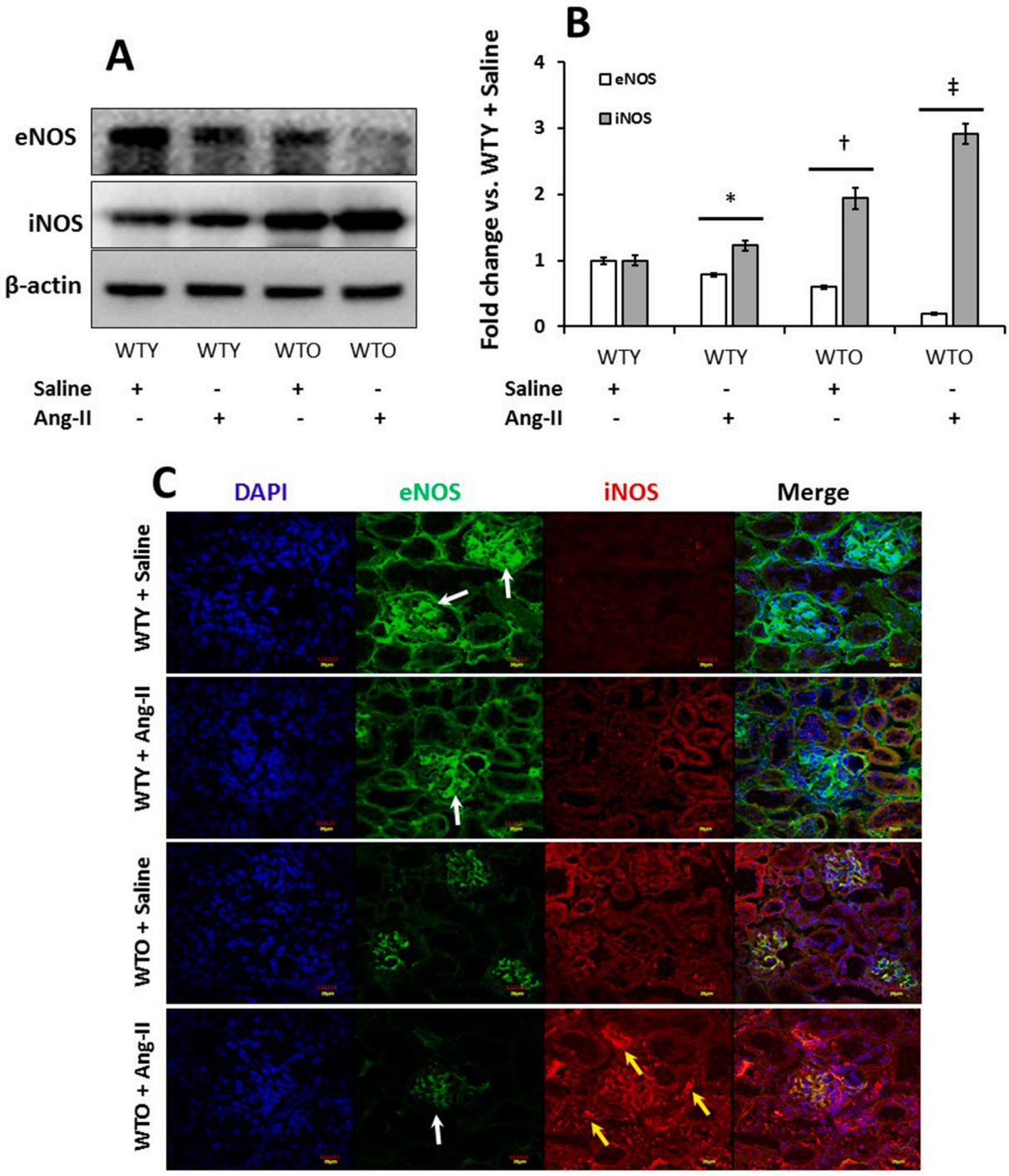

Fig. 8. Hypertension reduced eNOS and induced iNOS expression in old mice. Western blot analysis of kidney tissue obtained from mice treated without or with Ang-II. (A) The bands are showing expression of eNOS and iNOS in an equal amount of loaded proteins. Loading was normalized with β-actin. (B) The bar diagrams indicate densitometric analysis of protein bands and are presented as mean fold change ± SD (n = 5). Significant difference $^{*,\dagger}p < 0.05$ vs. WTY + Saline; $^{\ddagger}p < 0.05$ vs. other groups. (C) Immunostaining further confirmed that Ang-II downregulated eNOS (white arrows) and upregulated iNOS (yellow arrows) in aged mice. Representative images from eNOS and iNOS fluorescence stained kidney sections. (For interpretation of the references to color in this figure legend, the reader is referred to the Web version of this article.)

saline-treated mice (Fig. 5A-B) and worsened further following Ang-II treatment, which was about 3-fold higher than that in old mice receiving saline (Fig. 5A-B).

To further substantiate whether Ang-II aggravates oxidative stress in aged mice, we measured 4-HNE and reduced vs. oxidized glutathione (GSH:GSSG) ratio as surrogate indicators of oxidant stress. Our results indicated that 4-HNE and GSH remained at the baseline levels without any significant change in young animal treated Ang-II compared to young saline treated mice (Fig. 5C-D). GSSG, however, increased significantly in Ang-II treated young kidneys compared to young saline control (Fig. 5D). The levels of 4-HNE and GSSG increased significantly in old saline treated mice compared to young saline control (Fig. 5C-D) and increased further with Ang-II treatment compared to respective saline control and young mice groups with or without Ang-II (Fig. 5C-D).

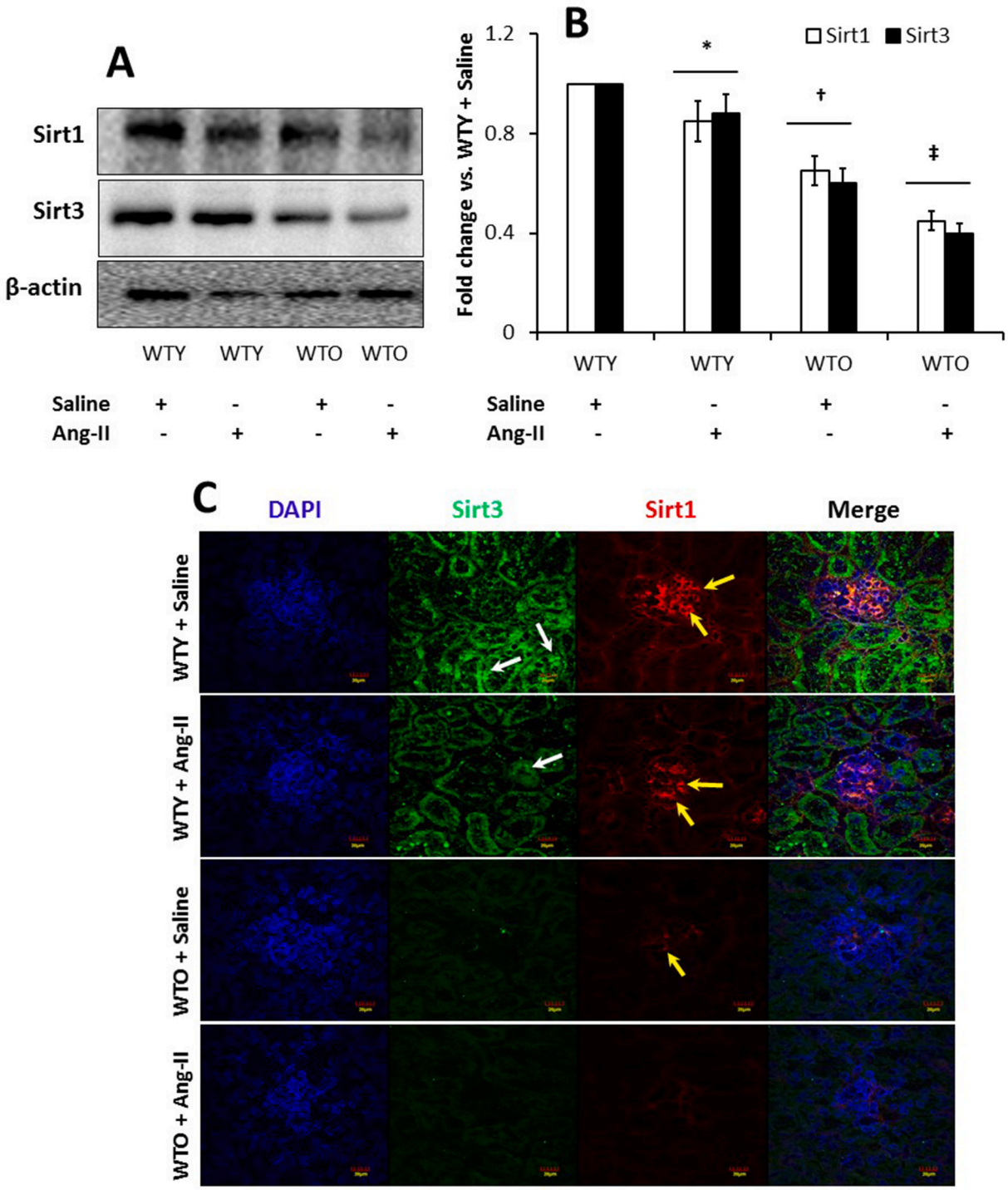

Fig. 9. Hypertension downregulated Sirt1 and Sirt3 in the aged kidney. (A) Proteins were isolated from the kidney tissue and were analyzed by Western blotting. An equal amount of protein was loaded onto each well, electrophoresed, and blotted. The expression of each protein was normalized with β-actin. (B) Bands were quantified by densitometry, and the bar diagram represents fold change vs. WTY control. Data represents mean ± SD (n = 5). Significant difference $^{*,\dagger}p < 0.05$ vs. WTY + Saline; $^{\ddagger}p < 0.05$ vs. other groups. (C) Representative images of Sirt1 and Sirt3 fluorescence staining in the kidney section. WTY mice demonstrated a high intensity of Sirt1 fluorescence in glomeruli (red) and Sirt3 in tubules (green). (For interpretation of the references to color in this figure legend, the reader is referred to the Web version of this article.)

The levels of GSH were diminished in old mice compared to young saline treated mice and decreased further with Ang-II (Fig. 5D).

3.6. *Nox4 and p22^{phox} were upregulated in aged hypertensive kidney*

NADPH oxidases are the major source of ROS production in CKD [26]. Among them, p22^{phox} and Nox4 are abundantly expressed in the kidney and upregulated in CKD [27]. To confirm ROS production as demonstrated in Fig. 5, we investigated whether Ang-II affects Nox4 and p22^{phox} expression in the kidney and if so, is there a differential expression in young vs. old. The Nox4 and p22^{phox} in the young mice treated with saline were considered as basal expression (Fig. 6A-B). Ang-II upregulated the expression of Nox4 and p22^{phox} in young mice compared to age-matched controls (Fig. 6A-B). Interestingly, the

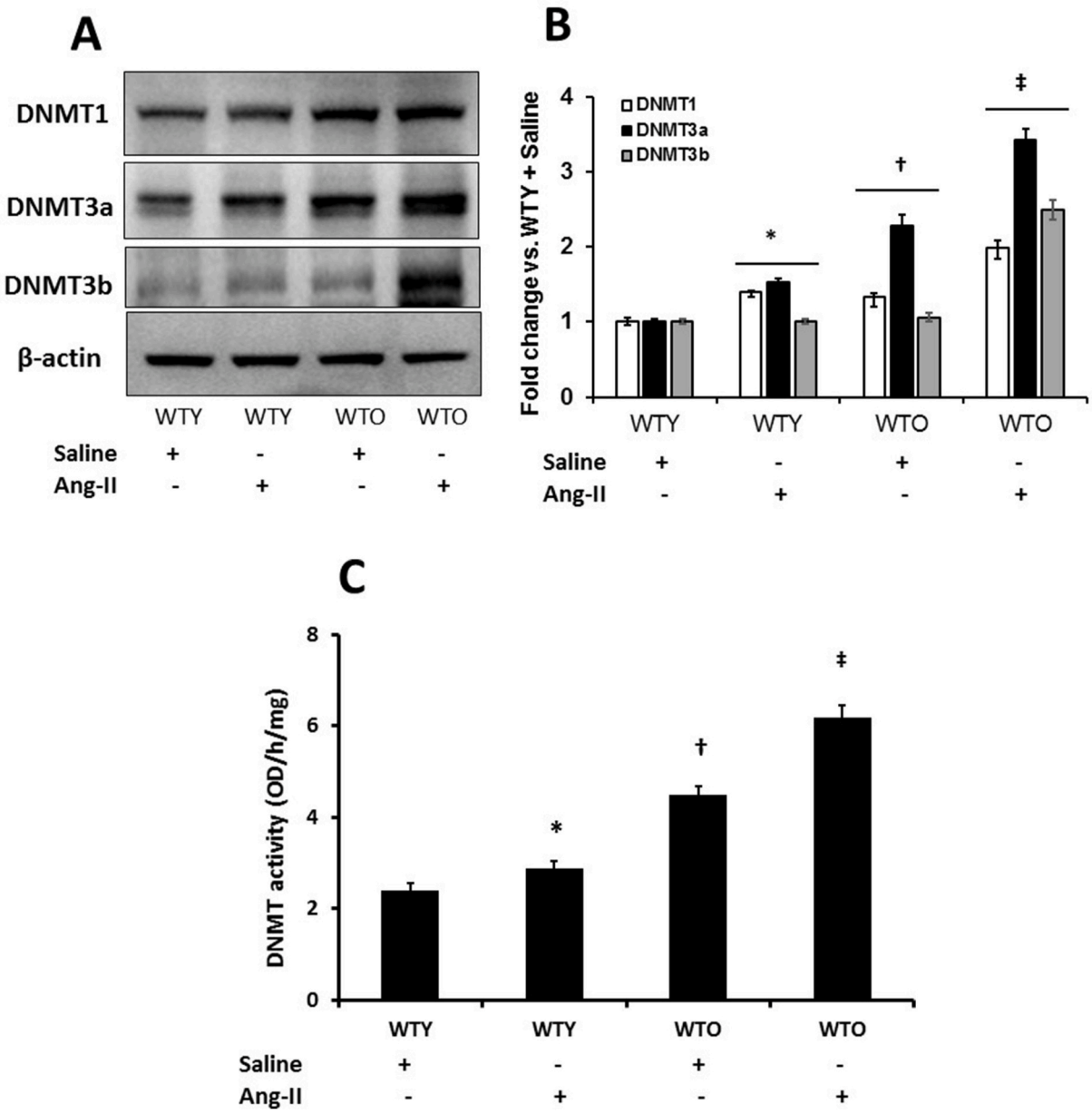

Fig. 10. Hypertension upregulated DNMTs in the aging kidney. (A) Kidney tissue was lysed, and protein expression was analyzed by Western blotting. An equal amount of protein was loaded onto each well, electrophoresed, transferred to a membrane, and immunoblotted with specific antibodies, as stated. Blots were re-probed with β-actin to demonstrate whether the protein was equally loaded. (B) Densitometric analyses were performed, and the fold changes of protein expression vs. WTY saline is presented as a bar diagram. (C) DNMT activity was measured as described in the methods. Values are mean ± SD (n = 5). Significance *, †$p < 0.05$ vs. WTY + Saline; ‡$p < 0.05$ vs. other groups.

expression of the two oxidases was significantly upregulated in old saline control compared to young control mice (Fig. 6A-B). Following Ang-II treatment, their expressions further increased compared to the other groups (Fig. 6A-B).

3.7. MnSOD, CuSOD, and catalase and their activities were downregulated in hypertensive aged kidney

Superoxide dismutase (SOD) catalyzes superoxide radical ($O_2^{\bullet-}$) into hydrogen peroxide (H_2O_2), which is broken down further into H_2O and O_2 by catalase [28]. To determine whether increased ROS in hypertension and aging was due to, in part, decreased MnSOD, CuSOD, and catalase, we measured these enzymes by Western blotting and immunostaining. Our results show that MnSOD, CuSOD, and catalase were abundantly expressed in WTY saline treated kidney, and were significantly downregulated with Ang-II (Fig. 7A-B). In the WTO saline treated mice, the expression of the enzymes was attenuated compared to WTY mice treated with saline. Following Ang-II treatment, the expression of the enzymes further diminished in old mice (Fig. 7A-B). Immunostaining kidney sections for MnSOD from WTY and WTO mice treated with or without Ang-II reflected similar findings as that seen in Western blotting (Fig. 7C).

We measured the activity of antioxidant enzymes, MnSOD, total SOD, and catalase to determine whether increased oxidative stress is a direct consequence of reduced enzyme activities. Our results show that MnSOD and total SOD, but not the catalase, activities were significantly decreased in WTY kidney treated with Ang-II compared to WTY control (Fig. 7D-E). In WTO saline treated kidney, all the enzymes activity were decreased significantly compared to WTY control. Following Ang-II treatment, the enzymatic activities of SODs and catalase were further

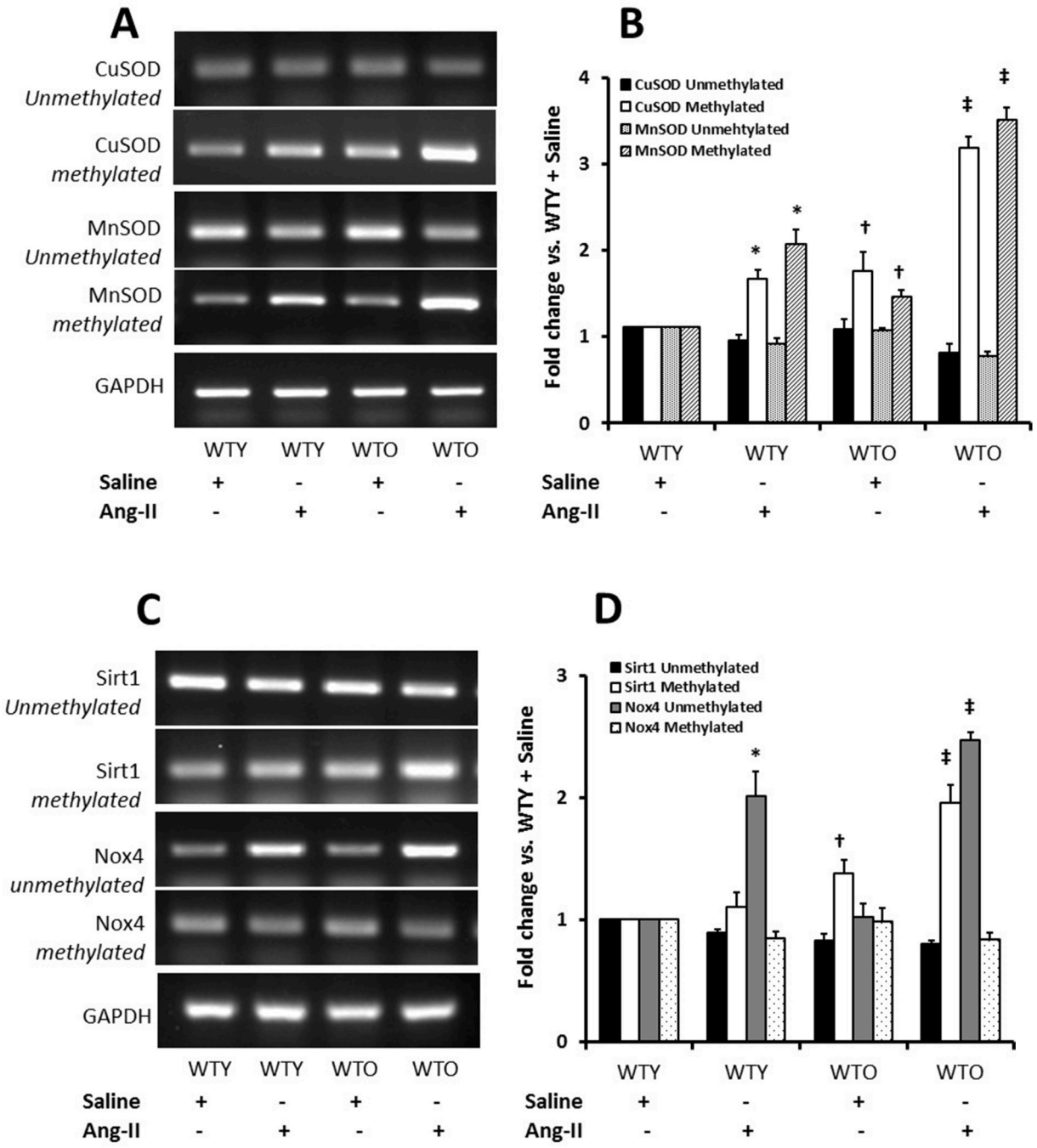

Fig. 11. Hypertension modulated methylation pattern of SODs, Nox4, and Sirt1 in the aging kidney. Tissue genomic DNA was extracted, and the methylation of DNA was measured by PCR analysis using methylation specific primers. PCR products of MnSOD, CuSOD, Nox4, and Sirt1 were subjected to agarose (2%) gel analysis. GAPDH was used as an internal standard to verify equal loading of PCR products. Methylated and unmethylated (A) MnSOD and CuSOD, and (B) Sirt1 and Nox4. (C) and (D) Methylated and unmethylated expression of the aforesaid genes were quantified by densitometry and expressed as fold change vs. WTY + Saline in the bar diagrams. Data represents mean ± SD (n = 5). Significance difference *, $^{\dagger}p < 0.05$ vs. WTY + Saline; $^{\ddagger}p < 0.05$ vs. other groups.

diminished in WTO mice compared to saline treated WTO group (Fig. 7D-E).

3.8. Downregulation of eNOS and upregulation of iNOS in hypertensive old kidney

In the young saline treated mice, eNOS was highly expressed and iNOS was minimal (Fig. 8A). Ang-II treatment in young mice reduced eNOS and upregulated iNOS expression compared to WTY saline control. In the WTO control kidney, the expression of eNOS was lower than in WTY saline treated group and iNOS was increased compared to respective young saline group (Fig. 8A-B). In WTO mice, Ang-II treatment further downregulated the expression of eNOS and iNOS was highly expressed compared to all the other groups (Fig. 8A-B). Immunostaining showed similar expression for eNOS (white arrows) and iNOS (yellow arrows) in the WTY and WTO with or without Ang-II treatment groups as seen in Western blotting (Fig. 8C).

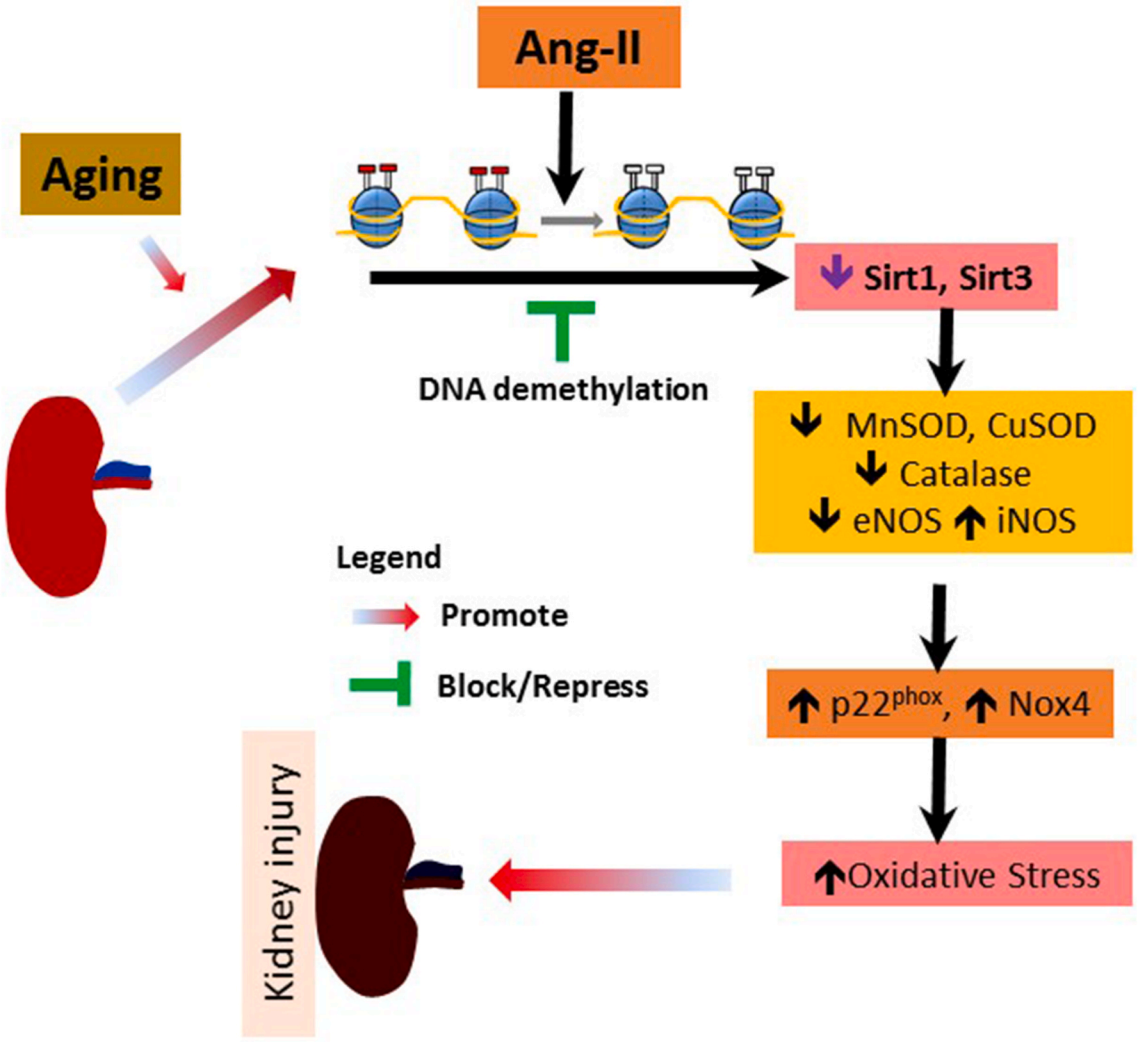

Fig. 12. Schematic of hypothesis and overall findings. Ang-II hypertension in aging causes hypermethylation of several oxidase/catalase enzymes leading to increased oxidative stress that promote kidney injury and remodeling.

3.9. Expression of Sirt1 and Sirt3 was reduced in aged and hypertensive mice

Sirt1 regulates various cellular processes involving antioxidant mechanisms [29], and Sirt3 is pivotal in reducing mitochondrial oxidative stress by limiting ROS production [30]. To determine whether Sirts have a role in hypertension and aging, we measured Sirt1 and Sirt3 by immunoblotting and immunostaining of the kidney tissue. Our results show basal expression of Sirt1 and Sirt3 in the WTY saline treated kidney and reduction with Ang-II treatment (Fig. 9A, B). In the WTO kidney, the expression of Sirt1 and Sirt3 was reduced compared to saline treated young mice and decreased further with Ang-II compared to the other groups (Fig. 9A-B). Similar results were observed with immunostaining of kidney sections for Sirt1 and Sirt3 (yellow and white arrows, respectively; Fig. 9C).

3.10. DNMTs were upregulated in Ang-II treated aged mice

We measured DNMT1, -3a, and -3b since the methyltransferases perform a variety of biological functions in mammalian cells [31,32]. The expression of the enzymes in WTY saline treated mice were considered basal (Fig. 10A-B). The expression of DNMT1 and -3a was upregulated, while -3b remained unaltered in WTY mice treated with Ang-II compared to WTY saline treatment group (Fig. 10A-B). In the WTO kidney, DNMT1, -3a, but not the -3b was upregulated compared to their respective expressions in the WTY saline controls (Fig. 10A-B). All three enzymes showed robust expression in WTO mice treated with Ang-II compared to WTO saline controls and WTY groups (Fig. 10A-B). We also measured DNMT activity by a colorimetric method (Fig. 10C). In the WTY saline treated mice, DNMT activity was at the basal level; whereas, Ang-II treatment significantly increased the activity (Fig. 10C). Compared to WTY control, the activity of DNMT was significantly increased in WTO saline treated mice. A further increase in the activity was observed in WTO animals following Ang-II (Fig. 10C).

3.11. Epigenetic DNA methylation pattern in Ang-II hypertension

We measured methylated and unmethylated CuSOD, MnSOD, Sirt1, and Nox4 gene expression in all groups. Unmethylated and methylated CuSOD in WTY control were considered as basal expression (Fig. 11A-B). There was no apparent change in the expression of unmethylated CuSOD in all the groups. In contrast, the expression of methylated CuSOD increased in Ang-II treated WTY and WTO mice; however, the increase was more robust in the WTO group compared to WTY (Fig. 11A-B). A similar trend was observed in the expression of unmethylated and methylated MnSOD in all the groups (Fig. 11A-B).

A non-significant decrease of unmethylated Sirt1 was observed in the control and Ang-II young mice groups. Ang-II treated old mice showed

decreased unmethylated Sirt1 compared to the other groups (Fig. 11C-D). Sirt1 methylation was increased in Ang-II treated young and old mice, but the increase was more robust in the old mice compared to the young mice (Fig. 11C-D). The unmethylated Nox4 levels were similar in WTY and WTO saline treatment groups. In contrast, unmethylated Nox4 increased significantly in Ang-II treated WTY mice compared to WTY saline treatment (Fig. 11C-D). A robust and significant increase in Nox4 unmethylated gene expression was observed in WTO treated with Ang-II compared to age-matched saline treatment group (Fig. 11C-D). The expression of methylated Nox4 gene remained relatively unchanged among all the groups (Fig. 11C-D).

4. Discussion

Oxidative stress results from redox imbalance caused by increased ROS production and reduced antioxidant reserve. In aging, increased oxidative damage causes organ injury and accelerates the development of hypertension by changing the vasculature phenotype. In addition, age-associated increase in oxidative stress initiates a series of molecular and vascular events resulting in pathophysiological changes and functional deterioration in the kidney. However, the mechanisms regulating oxidative and anti-oxidative enzymes in the kidney during aging and hypertension remains unclear. The present study examined the role of DNA methylation of the enzymes involved in redox balance in hypertension-induced aged kidney injury. Our study revealed that the old mice were vulnerable to develop hypertension compared to young in response to Ang-II (Fig. 1). This is in part due to changes in renal vasculature, such as increased renal artery resistance, reduced vascular density, and blood flow in the renal cortex (Figs. 2–4).

Oxidative stress and the resultant cellular dysfunction are considered as a major driver of many vascular disease states [33]. Besides, previous studies have indicated that increased oxidative stress and ROS production is a causal factor of the aging process [34]. In our study, we measured superoxide using DHE assay (Fig. 5A). It is, however, reported that intracellular superoxide-specific products i.e., 2-OH-E^+ as a reaction between superoxide and DHE could not be definitely assessed using fluorescence base microscopic assays [35,36]. Therefore, we measured 4-HNE and GSH to GSSG ratio, in addition to DHE based superoxide detection, to estimate overall oxidative stress in the tissue samples. Our results revealed a significant increase of oxidative stress markers, particularly superoxide, 4-HNE, and decreased ratio of GSH/GSSG in old mice treated with Ang-II compared to the young with the same Ang-II regimen (Fig. 5). The production of ROS, particularly superoxide, is largely regulated by a membrane-bound enzyme complex, NADPH oxidase (Nox). As such, the Nox family has been demonstrated to be a crucial mediator of the pathological changes in the vasculature [37]. There are seven Nox isoforms that include Nox1-5 and Duox1-2, and components of Noxs' are $p67^{phox}$, $p47^{phox}$, $p40^{phox}$, $p22^{phox}$, RAC1, RAC2, Noxo1, and Noxa1 [38]. Nox4 is the major NADPH oxidase isoform in the kidney, and it contributes to redox processes that are involved in several kidney diseases, including hypertensive nephropathy [39]. The activation of Nox4 does not require interaction with the classic NADPH oxidase cytosolic subunits ($p47^{phox}$, $p76^{phox}$, $p40^{phox}$) but it requires $p22^{phox}$ [14,40]. We, therefore, quantified the expression of Nox4 and $p22^{phox}$ that showed maximum expression in the old mice (Fig. 6), suggesting a strong correlation and causal relationship for both proteins for increased ROS production during age-associated hypertension.

The role of Nox4 in the vasculature remains controversial since both deleterious and protective effects have been reported in vascular diseases and have been extensively discussed in a recent publication [41]. The protective role of Nox4 is supported by studies that demonstrated angiogenesis [42], anti-inflammatory, and anti-remodeling mechanisms [43]. Evidence shows that Nox4 facilitates angiogenesis and recovery from hypoxia via activating endothelial nitric oxide synthase (eNOS) to increase the bioavailability of vasodilator NO, production of H_2O_2, a putative endothelium-derived vasorelaxing factor, and expression of Nrf-2, a master regulator of antioxidant gene for activation of antioxidant systems [42]. On the other hand, pathogenic roles for Nox4 have been demonstrated in several studies. In in vitro study Ang-II was shown to uncouple eNOS, reduce NO bioavailability, and activate the production of ROS [44]. In salt-sensitive rats, Nox4 upregulation was associated with excess tubular injury and reduced NADH/NAD ratio [45]. Others have demonstrated that Nox4 upregulation in salt-sensitive rats increased H_2O_2 production and early ENaC activity indicating increased Na absorption that contributes to the development and progression of hypertension [46]. In our study, we have seen increased global expression of Nox4 in the kidney (Fig. 6) with a concomitant increase in oxidative stress (Fig. 5) in Ang-II hypertension, suggesting a pathological role of Nox4 in kidney injury, especially in aged mice. Further studies are required to delineate and confirm the underlying signaling mechanisms that direct the pathogenesis in aged mice.

The family of superoxide dismutase consists of MnSOD and Cu/ZnSOD and extracellular dismutases. They are antioxidant enzymes with the ability to detoxify cellular free radicals to produce H_2O_2 and molecular oxygen [47]. Subsequently, catalase, a tetrameric enzyme, breaks down H_2O_2 into water and oxygen [48]. Thus, these enzymes are important machinery in protecting cells from oxidative stress-mediated damage under pathological conditions, particularly age-associated pathology [49–51]. Corroborating with these previous reports, we observed reduced expression of MnSOD, CuSOD, and catalase in the aged mice compared to young (Fig. 7A-C). The enzymes' expression further diminished with Ang-II-induced hypertension. More importantly, diminished antioxidant enzymatic activities of MnSOD, total SOD, and catalase suggest an apparent vulnerability of aged mice to ROS-induced injury (Fig. 7D-E). Interestingly, the production of nitric oxide (NO) metabolites was found to be increased in an assay where Cu-ZnSOD was added in a reaction containing L-NAME [52], suggesting that there might be a correlation between diminished expression of antioxidant enzymes and NO producing enzymes in our experimental hypertensive aging model. Therefore, we measured the expression of eNOS and iNOS expression in our experimental samples, and the results are discussed below in the context of current information.

The nitric oxide synthases (NOSs) are a family of enzymes with the ability to catalyze the generation of NO from L-arginine. Endothelial nitric oxide synthase (eNOS) and inducible nitric oxide synthase (iNOS) are two main isoforms in the family of NOS enzymes in the vascular beds. The eNOS is mainly responsible for producing NO in the vascular endothelium, which is essential for cardiovascular functions, including blood vessels dilation and thus modulates blood pressure, and performs other vasoprotective and anti-atherosclerotic effects [53]. However, eNOS can also function deleteriously in a state of oxidative environment, where increased superoxide anions (O_2^-) react with NO to generate peroxynitrite ($ONOO^-$) leading to further oxidative damage by oxidizing protein, thiol, and tyrosine nitration [54]. These processes not only limit NO availability but also lead to NOS uncoupling [55]. Consequently, uncoupled eNOS produces O_2^- instead of NO, which could cause additional deterioration of vascular function [56]. On the other hand, induction of iNOS occurs in an oxidative environment and is typically upregulated in inflammatory diseases and plays a role in anti-microbial and anti-tumor activities as part of the oxidative macrophage outburst [57]. Hence, high-output iNOS can be considered as an indicator of oxidative stress. To determine whether a shift of induction from eNOS to iNOS expression has occurred in our study, we measured these enzymes in all the groups. Our results indicate that eNOS expression is decreased in the aged mice and worsens further in response to Ang-II-induced hypertension (Fig. 8A-C). The changes are associated with increased expression of iNOS. Together, these results suggest a shift from eNOS to iNOS induction worsening the oxidative environment in the aged mice with Ang-II insult.

Epigenetic changes are considered as an important aspect of the aging process, and Sirtuins (Sirts) play an important role in epigenetic modifications to modulate the aging process. Sirt1 functions to regulate

various cellular processes involving antioxidant mechanisms, cell survival, cell cycling, cell differentiation, and metabolism by deacetylation of target molecules [29]. A recent study has indicated that eNOS activity is induced through Sirt1 upregulation, which may inhibit oxidative-dependent endothelial senescence [58]. On the other hand, Sirt3 is pivotal in maintaining mitochondrial function via limiting oxidative stress and decreasing the production of ROS with a reduction in mitochondrial membrane potential [30]. In addition, mitochondrial localization of Sirt3 exhibited vasoprotective effects by promoting the mitochondrial antioxidant defense system [59]. Corroborating with these previous reports, our results suggest a diminished expression of Sirt1 and 3 (Fig. 9A-C) is possibly related to decreasing MnSOD, CuSOD, and catalase that resulted in an upregulation of ROS implying that aged hypertensive mice had attenuated antioxidant defense system.

Methylation of DNA performs a wide variety of biological functions, and the DNA methyltransferase (DNMT) family is responsible for transferring a methyl group to DNA. Alterations in the DNA methylation status in genes have been linked with the development of hypertension. For example, the *AT1a* receptor gene in the vasculature was upregulated by promoter hypomethylation in the development of genetic hypertension [60]. Others have shown that methylation of the promoter of the *HSD11B2* gene plays a role in developing hypertension [61]. DNMT1 is a maintenance methyltransferase that adds DNA with a methyl group when one strand is already methylated [62]. In contrast, DNMT3a and 3b recognize unmethylated or hemimethylated DNA to perform *de novo* methylation to assist in maintenance [63]. In the present study, we measured DNMT1, 3a, and 3b, and the results indicate that maintenance methylation enzyme DNMT1, was upregulated in hypertensive young as well as old animals with Ang-II infusion compared to normotensive young mice (Fig. 10A-B). The expression of DNMT3a increased significantly in young animals with Ang-II compared to control animals. DNMT3a was increased in old animals treated without or with Ang-II compared to young control animals (Fig. 10A-B). A similar trend in the expression of DNMT3b was also observed in the young group with Ang-II, and in old groups with or without Ang-II compared to young alone (Fig. 10A-B). The results from the DNMT assay also suggest that in old animals, the DNMT activity was increased compared to young and further increases in response to Ang-II (Fig. 10C). Methylation specific PCR for CuSOD, MnSOD, and Sirt1 showed increased methylation in aged mice and to Ang-II treatment compared to young mice suggesting gene suppression (Fig. 11A-D). In contrast, Ang-II-induced hypertension showed increased unmethylated Nox4 suggesting increased gene expression (Fig. 11C-D). The methylation pattern above corroborated with the protein expression in the kidney. Our results thus suggest that epigenetic methylation played a role in oxidative stress response in aging and hypertension. Of note, DNA hypermethylation typically represses gene transcription, and our results corroborate with SODs and Sitr1 protein expression with DNA methylation pattern.

In summary, NADPH oxidases $p22^{phox}$ and Nox4 were upregulated in the senescent kidney in response to Ang-II. These changes were associated with decreased SODs, catalase, Sirt1, and -3 along with an imbalance in eNOS/iNOS expression that increased oxidative stress. The alteration in DNMTs expression and methylation pattern of the genes above indicate that epigenetic mechanisms contribute to the hypertensive injury in the aged kidney. The overall findings and a possible pathway is presented in Fig. 12. In order to further delineate and potentially target the epigenetic mechanisms in hypertension injury of the aged kidney, more studies are required to understand the other players that include histone/protein posttranslational modifications and the role of non-coding RNA. A significant cross-talk may exist between the different mechanisms to regulate redox balance.

Funding sources

This work was supported in part by National Institutes of Health Grants, DK104653 and DK116591 (to U.S.), and American Heart Association Scientist Development Grant, 15SDG25840013 (to S.P.)

Authors' contributions

SP and LR conceived the idea, designed and performed the experiments, analyzed the data, interpreted the results, prepared figures, and drafted the manuscript; SKJ, SM and RK contributed to the experiments; US interpreted the results, edited, and approved final version of the manuscript.

Declaration of competing interest

The authors declare no conflicts of interest, financial or otherwise.

Acknowledgments

We thank Naira Metreveli for technical assistance and for setting up animal experiments during the course of this study.

References

[1] U.S. Health, End-stage Renal Disease Patients, by Selected Characteristics: United States, Selected Years 1980–2010, Centers for Disease Control and Prevention, 2011. www.cdc.gov/nchs/data/hus/2011/051.pdf.
[2] P.M. Kearney, M. Whelton, K. Reynolds, P. Muntner, P.K. Whelton, J. He, Global burden of hypertension: analysis of worldwide data, Lancet 365 (2005) 217–223.
[3] Z. Sun, Aging, arterial stiffness, and hypertension, Hypertension 65 (2015) 252–256.
[4] G.M. Martin, The biology of aging: 1985–2010 and beyond, Faseb. J. 25 (2011) 3756–3762.
[5] K.B. Beckman, B.N. Ames, The free radical theory of aging matures, Physiol. Rev. 78 (1998) 547–581.
[6] M.C. Haigis, B.A. Yankner, The aging stress response, Mol. Cell 40 (2010) 333–344.
[7] R.S. Sohal, R. Weindruch, Oxidative stress, caloric restriction, and aging, Science 273 (1996) 59–63.
[8] G. Barja, Updating the mitochondrial free radical theory of aging: an integrated view, key aspects, and confounding concepts, Antioxidants Redox Signal. 19 (2013) 1420–1445.
[9] N. Sinha, P.K. Dabla, Oxidative stress and antioxidants in hypertension-a current review, Curr. Hypertens. Rev. 11 (2015) 132–142.
[10] L.K. Lee, T.W. Meyer, A.S. Pollock, D.H. Lovett, Endothelial cell injury initiates glomerular sclerosis in the rat remnant kidney, J. Clin. Invest. 96 (1995) 953–964.
[11] S.L. Berger, T. Kouzarides, R. Shiekhattar, A. Shilatifard, An operational definition of epigenetics, Genes Dev. 23 (2009) 781–783.
[12] H. Wang, X. Chen, Y. Su, P. Paueksakon, W. Hu, M.Z. Zhang, R.C. Harris, T. S. Blackwell, R. Zent, A. Pozzi, p47(phox) contributes to albuminuria and kidney fibrosis in mice, Kidney Int. 87 (2015) 948–962.
[13] J.D. Lambeth, NOX enzymes and the biology of reactive oxygen, Nat. Rev. Immunol. 4 (2004) 181–189.
[14] A.C. Montezano, D. Burger, G.S. Ceravolo, H. Yusuf, M. Montero, R.M. Touyz, Novel Nox homologues in the vasculature: focusing on Nox4 and Nox5, Clin. Sci. 120 (2011) 131–141.
[15] S. Cuevas, Y. Zhang, Y. Yang, C. Escano, L. Asico, J.E. Jones, I. Armando, P.A. Jose, Role of renal DJ-1 in the pathogenesis of hypertension associated with increased reactive oxygen species production, Hypertension 59 (2012) 446–452.
[16] C.J. Weydert, J.J. Cullen, Measurement of superoxide dismutase, catalase and glutathione peroxidase in cultured cells and tissue, Nat. Protoc. 5 (2010) 51–66.
[17] A.R. Subauste, C.F. Burant, Role of FoxO1 in FFA-induced oxidative stress in adipocytes, Am. J. Physiol. Endocrinol. Metabol. 293 (2007) E159–E164.
[18] C.K. Singh, G. Chhabra, M.A. Ndiaye, L.M. Garcia-Peterson, N.J. Mack, N. Ahmad, The role of sirtuins in antioxidant and redox signaling, Antioxidants Redox Signal. 28 (2018) 643–661.
[19] P. Liu, Y. Liu, H. Liu, X. Pan, Y. Li, K. Usa, M.K. Mishra, J. Nie, M. Liang, Role of DNA de Novo (De)Methylation in the kidney in salt-induced hypertension, Hypertension 72 (2018) 1160–1171.
[20] I. Smolarek, E. Wyszko, A.M. Barciszewska, S. Nowak, I. Gawronska, A. Jablecka, M.Z. Barciszewska, Global DNA methylation changes in blood of patients with essential hypertension, Med. Sci. Mon. Int. Med. J. Exp. Clin. Res. 16 (2010) CR149–155.
[21] S.B. Pushpakumar, S. Kundu, N. Metreveli, U. Sen, Folic acid mitigates angiotensin-II-induced blood pressure and renal remodeling, PloS One 8 (2013), e83813.
[22] S.B. Pushpakumar, S. Kundu, N. Metreveli, S.C. Tyagi, U. Sen, Matrix metalloproteinase inhibition mitigates renovascular remodeling in salt-sensitive hypertension, Physiol. Rep. 1 (2013), e00063.
[23] S.B. Pushpakumar, S. Kundu, T. Pryor, S. Givvimani, E. Lederer, S.C. Tyagi, U. Sen, Angiotensin-II induced hypertension and renovascular remodelling in tissue inhibitor of metalloproteinase 2 knockout mice, J. Hypertens. 31 (2013) 2270–2281.

[24] S. Pushpakumar, L. Ren, S. Kundu, A. Gamon, S.C. Tyagi, U. Sen, Toll-like receptor 4 deficiency reduces oxidative stress and macrophage mediated inflammation in hypertensive kidney, Sci. Rep. 7 (2017) 6349.
[25] S. Pushpakumar, S. Kundu, N. Narayanan, U. Sen, DNA hypermethylation in hyperhomocysteinemia contributes to abnormal extracellular matrix metabolism in the kidney, Faseb. J. 29 (2015) 4713–4725.
[26] M. Munoz, M.E. Lopez-Oliva, C. Rodriguez, M.P. Martinez, J. Saenz-Medina, A. Sanchez, B. Climent, S. Benedito, A. Garcia-Sacristan, L. Rivera, M. Hernandez, D. Prieto, Differential contribution of Nox1, Nox2 and Nox4 to kidney vascular oxidative stress and endothelial dysfunction in obesity, Redox Biol. 28 (2019) 101330.
[27] H. Watanabe, Y. Miyamoto, D. Honda, H. Tanaka, Q. Wu, M. Endo, T. Noguchi, D. Kadowaki, Y. Ishima, S. Kotani, M. Nakajima, K. Kataoka, S. Kim-Mitsuyama, M. Tanaka, M. Fukagawa, M. Otagiri, T. Maruyama, p-Cresyl sulfate causes renal tubular cell damage by inducing oxidative stress by activation of NADPH oxidase, Kidney Int. 83 (2013) 582–592.
[28] S. Dieterich, U. Bieligk, K. Beulich, G. Hasenfuss, J. Prestle, Gene expression of antioxidative enzymes in the human heart: increased expression of catalase in the end-stage failing heart, Circulation 101 (2000) 33–39.
[29] Y. Horio, T. Hayashi, A. Kuno, R. Kunimoto, Cellular and molecular effects of sirtuins in health and disease, Clin. Sci. 121 (2011) 191–203.
[30] T. Shi, F. Wang, E. Stieren, Q. Tong, SIRT3, a mitochondrial sirtuin deacetylase, regulates mitochondrial function and thermogenesis in brown adipocytes, J. Biol. Chem. 280 (2005) 13560–13567.
[31] Y. Liu, X. Tian, S. Liu, D. Liu, Y. Li, M. Liu, X. Zhang, C. Yan, Y. Han, DNA hypermethylation: a novel mechanism of CREG gene suppression and atherosclerogenic endothelial dysfunction, Redox Biol. (2020) 101444.
[32] X. Zhu, D. Li, Y. Du, W. He, Y. Lu, DNA hypermethylation-mediated downregulation of antioxidant genes contributes to the early onset of cataracts in highly myopic eyes, Redox Biol. 19 (2018) 179–189.
[33] G. Gavazzi, B. Banfi, C. Deffert, L. Fiette, M. Schappi, F. Herrmann, K.H. Krause, Decreased blood pressure in nox1-deficient mice, FEBS Lett. 580 (2006) 497–504.
[34] C. Cencioni, F. Spallotta, F. Martelli, S. Valente, A. Mai, A.M. Zeiher, C. Gaetano, Oxidative stress and epigenetic regulation in ageing and age-related diseases, Int. J. Mol. Sci. 14 (2013) 17643–17663.
[35] J. Zielonka, B. Kalyanaraman, Hydroethidine- and MitoSOX-derived red fluorescence is not a reliable indicator of intracellular superoxide formation: another inconvenient truth, Free Radic. Biol. Med. 48 (2010) 983–1001.
[36] J. Zielonka, B. Kalyanaraman, Small-molecule luminescent probes for the detection of cellular oxidizing and nitrating species, Free Radic. Biol. Med. 128 (2018) 3–22.
[37] C. Kleinschnitz, H. Grund, K. Wingler, M.E. Armitage, E. Jones, M. Mittal, D. Barit, T. Schwarz, C. Geis, P. Kraft, K. Barthel, M.K. Schuhmann, A.M. Herrmann, S. G. Meuth, G. Stoll, S. Meurer, A. Schrewe, L. Becker, V. Gailus-Durner, H. Fuchs, T. Klopstock, M.H. de Angelis, K. Jandeleit-Dahm, A.M. Shah, N. Weissmann, H. H. Schmidt, Post-stroke inhibition of induced NADPH oxidase type 4 prevents oxidative stress and neurodegeneration, PLoS Biol. 8 (2010), e1000479.
[38] A. Panday, M.K. Sahoo, D. Osorio, S. Batra, NADPH oxidases: an overview from structure to innate immunity-associated pathologies, Cell. Mol. Immunol. 12 (2015) 5–23.
[39] Q. Yang, F.R. Wu, J.N. Wang, L. Gao, L. Jiang, H.D. Li, Q. Ma, X.Q. Liu, B. Wei, L. Zhou, J. Wen, T.T. Ma, J. Li, X.M. Meng, Nox4 in renal diseases: an update, Free Radic. Biol. Med. 124 (2018) 466–472.
[40] M. Geiszt, J.B. Kopp, P. Várnai, T.L. Leto, Identification of Renox, an NAD(P)H oxidase in kidney, Proc. Natl. Acad. Sci. U.S.A. 97 (2000) 8010–8014.
[41] R.D. Rajaram, R. Dissard, V. Jaquet, S. de Seigneux, Potential benefits and harms of NADPH oxidase type 4 in the kidneys and cardiovascular system, Nephrol. Dial. Transplant. 34 (2019) 567–576.
[42] S.M. Craige, K. Chen, Y. Pei, C. Li, X. Huang, C. Chen, R. Shibata, K. Sato, K. Walsh, J.F.J. Keaney, NADPH oxidase 4 promotes endothelial angiogenesis through endothelial nitric oxide synthase activation, Circulation 124 (2011) 731–740.
[43] M.U. Moreno, I. Gallego, B. López, A. González, A. Fortuño, S.J. G, F. Valencia, J. J. Gómez-Doblas, E. de Teresa, A.M. Shah, J. Díez, G. Zalba, Decreased Nox4 levels in the myocardium of patients with aortic valve stenosis, Clin. Sci. 125 (2013) 291–300.
[44] D.Y. Lee, F. Wauquier, A.A. Eid, L.J. Roman, G. Ghosh-Choudhury, K. Khazim, K. Block, Y. Gorin, Nox4 NADPH oxidase mediates peroxynitrite-dependent uncoupling of endothelial nitric-oxide synthase and fibronectin expression in response to angiotensin II: role of mitochondrial reactive oxygen species, J. Biol. Chem. 288 (2013) 28668–28686.
[45] A.W. Cowley Jr., C. Yang, N.N. Zheleznova, A. Staruschenko, T. Kurth, L. Rein, V. Kumar, K. Sadovnikov, A. Dayton, M. Hoffman, R.P. Ryan, M.M. Skelton, F. Salehpour, M. Ranji, A. Geurts, Evidence of the importance of Nox4 in production of hypertension in dahl salt-sensitive rats, Hypertension 67 (2016) 440–450.
[46] T.S. Pavlov, O. Palygin, E. Isaeva, V. Levchenko, S. Khedr, G. Blass, D. V. Ilatovskaya, A.W. Cowley Jr., A. Staruschenko, NOX4-dependent regulation of ENaC in hypertension and diabetic kidney disease, Faseb. J. 34 (2020) 13396–13408.
[47] S. Miriyala, I. Spasojevic, A. Tovmasyan, D. Salvemini, Z. Vujaskovic, D. St Clair, I. Batinic-Haberle, Manganese superoxide dismutase, MnSOD and its mimics, Biochim. Biophys. Acta 1822 (2012) 794–814.
[48] K.R. Olson, Y. Gao, E.R. DeLeon, M. Arif, F. Arif, N. Arora, K.D. Straub, Catalase as a sulfide-sulfur oxido-reductase: an ancient (and modern?) regulator of reactive sulfur species (RSS), Redox Biol. 12 (2017) 325–339.
[49] N. Basisty, D.F. Dai, A. Gagnidze, L. Gitari, J. Fredrickson, Y. Maina, R.P. Beyer, M. J. Emond, E.J. Hsieh, M.J. MacCoss, G.M. Martin, P.S. Rabinovitch, Mitochondrial-targeted catalase is good for the old mouse proteome, but not for the young: 'reverse' antagonistic pleiotropy? Aging Cell 15 (2016) 634–645.
[50] H.B. Kwak, Y. Lee, J.H. Kim, H. Van Remmen, A.G. Richardson, J.M. Lawler, MnSOD overexpression reduces fibrosis and pro-apoptotic signaling in the aging mouse heart, J. Gerontol. Series A, Biol. Sci. Med. Sci. 70 (2015) 533–544.
[51] A.R. Robinson, M.J. Yousefzadeh, T.A. Rozgaja, J. Wang, X. Li, J.S. Tilstra, C. H. Feldman, S.Q. Gregg, C.H. Johnson, E.M. Skoda, M.C. Frantz, H. Bell-Temin, H. Pope-Varsalona, A.U. Gurkar, L.A. Nasto, R.A.S. Robinson, H. Fuhrmann-Stroissnigg, J. Czerwinska, S.J. McGowan, N. Cantu-Medellin, J.B. Harris, S. Maniar, M.A. Ross, C.E. Trussoni, N.F. LaRusso, E. Cifuentes-Pagano, P. J. Pagano, B. Tudek, N.V. Vo, L.H. Rigatti, P.L. Opresko, D.B. Stolz, S.C. Watkins, C. E. Burd, C.M.S. Croix, G. Siuzdak, N.A. Yates, P.D. Robbins, Y. Wang, P. Wipf, E. E. Kelley, L.J. Niedernhofer, Spontaneous DNA damage to the nuclear genome promotes senescence, redox imbalance and aging, Redox Biol. 17 (2018) 259–273.
[52] T. Liu, M. Zhang, G.T. Mukosera, D. Borchardt, Q. Li, T.E. Tipple, A.S. Ishtiaq Ahmed, G.G. Power, A.B. Blood, L-NAME releases nitric oxide and potentiates subsequent nitroglycerin-mediated vasodilation, Redox Biol. 26 (2019) 101238.
[53] U. Förstermann, W.C. Sessa, Nitric oxide synthases: regulation and function, Eur. Heart J. 33 (2012) 829–837.
[54] S. Bartesaghi, R. Radi, Fundamentals on the biochemistry of peroxynitrite and protein tyrosine nitration, Redox Biol. 14 (2018) 618–625.
[55] G. Gavazzi, C. Deffert, C. Trocme, M. Schappi, F.R. Herrmann, K.H. Krause, NOX1 deficiency protects from aortic dissection in response to angiotensin II, Hypertension 50 (2007) 189–196.
[56] A.V. Santhanam, L.V. d'Uscio, L.A. Smith, Z.S. Katusic, Uncoupling of eNOS causes superoxide anion production and impairs NO signaling in the cerebral microvessels of hph-1 mice, J. Neurochem. 122 (2012) 1211–1218.
[57] I.N. Mungrue, M. Husain, D.J. Stewart, The role of NOS in heart failure: lessons from murine genetic models, Heart Fail. Rev. 7 (2002) 407–422.
[58] H. Ota, M. Eto, M.R. Kano, T. Kahyo, M. Setou, S. Ogawa, K. Iijima, M. Akishita, Y. Ouchi, Induction of endothelial nitric oxide synthase, SIRT1, and catalase by statins inhibits endothelial senescence through the Akt pathway, Arterioscler. Thromb. Vasc. Biol. 30 (2010) 2205–2211.
[59] P.C. Tseng, S.M. Hou, R.J. Chen, H.W. Peng, C.F. Hsieh, M.L. Kuo, M.L. Yen, Resveratrol promotes osteogenesis of human mesenchymal stem cells by upregulating RUNX2 gene expression via the SIRT1/FOXO3A axis, J. Bone Miner. Res. 26 (2011) 2552–2563.
[60] F. Pei, X. Wang, R. Yue, C. Chen, J. Huang, J. Huang, X. Li, C. Zeng, Differential expression and DNA methylation of angiotensin type 1A receptors in vascular tissues during genetic hypertension development, Mol. Cell. Biochem. 402 (2015) 1–8.
[61] S. Friso, F. Pizzolo, S.W. Choi, P. Guarini, A. Castagna, V. Ravagnani, A. Carletto, P. Pattini, R. Corrocher, O. Olivieri, Epigenetic control of 11 beta-hydroxysteroid dehydrogenase 2 gene promoter is related to human hypertension, Atherosclerosis 199 (2008) 323–327.
[62] A. Hermann, R. Goyal, A. Jeltsch, The Dnmt1 DNA-(cytosine-C5)-methyltransferase methylates DNA processively with high preference for hemimethylated target sites, J. Biol. Chem. 279 (2004) 48350–48359.
[63] J. Liao, R. Karnik, H. Gu, M.J. Ziller, K. Clement, A.M. Tsankov, V. Akopian, C. A. Gifford, J. Donaghey, C. Galonska, R. Pop, D. Reyon, S.Q. Tsai, W. Mallard, J. K. Joung, J.L. Rinn, A. Gnirke, A. Meissner, Targeted disruption of DNMT1, DNMT3A and DNMT3B in human embryonic stem cells, Nat. Genet. 47 (2015) 469–478.